1970

A digital simulation for optimum nonlinear detection of binary signals in impulsive noise

Ralph Bernard Fluchel

Department:

A DIGITAL SIMULATION FOR OPTIMUM NONLINEAR DETECTION OF BINARY SIGNALS IN IMPULSIVE NOISE

BY

RALPH BERNARD FLUCHEL, 1945-

A THESIS

Presented to the Faculty of the Graduate School of the

UNIVERSITY OF MISSOURI-ROLLA

In Partial Fulfillment of the Requirements for the Degree

MASTER OF SCIENCE IN ELECTRICAL ENGINEERING

1970

Approved by

R. E. Fluchel (Advisor) David C. Cunningham

R. J. Perico

ABSTRACT

The problem of reducing the effects of impulsive noise on binary communication systems is considered. A digital simulation of such a system is developed in order to find a nearly optimum (minimum probability of error criterion) nonlinear device to precede detection. The level of the Gaussian noise power is found to be the most important parameter for determining the nearly optimum nonlinear device.

ACKNOWLEDGEMENT

The author would like to express his appreciation to Dr. Roger E. Ziemer for suggesting this topic and for his assistance during this project.

TABLE OF CONTENTS

LIST OF ILLUSTRATIONS

LIST OF TABLES

I. INTRODUCTION

The problem of detection of a known signal in additive Gaussian noise has received a great deal of attention in the literature and the optimum detector structure is well known for this case. However, detection of signals in non-Gaussian noise has received much less attention mainly because of the mathematical difficulties involved. Consequently, optimum detector structures have been found only for a few special cases involving non-Gaussian noise.

Impulsive noise is a particular type of non-Gaussian noise which is characterized by randomly occurring noise spikes of large amplitude which may be approximated as impulses. In radio, atmospheric noise is largely impulsive in nature. Impulsive noise also occurs in wire links due to such things as lightning and switching transients [1]. This thesis will deal with the performance of a digital communications system in the presence of impulsive noise. More specifically, it will deal with matched filter detection of phase-shift keyed (PSK) signals in the presence of additive impulsive and Gaussian noise. A reasonably good, or nearly optimum, nonlinearity preceding the matched filter will be found. Before giving a more precise statement of the problem, the pertinent literature will be summarized.

II. REVIEW OF LITERATURE

Not a great deal of work has been done in the area of impulsive noise. Halsted [2] calculated bit error probabilities for an autocorrelation receiver for binary data. Engel [3] has calculated the average number of errors per noise burst for a number of digital modulation systems. He takes into account the effects of filtering on the signal and noise. Lindenlaub and Chen [4] analyzed the performance of binary matched filter receivers in impulsive noise. Ziemer [5] has calculated the probability of character error for M-ary digital communications systems. The receiver considered was the matched filter receiver and a number of modulation schemes were considered. Ziemer [6] also has calculated the probability of error for binary PSK and M-ary ASK (Amplitude Shift Keying) for additive combinations of impulsive and Gaussian noise. More recently, Bello and Esposito [1] have developed a method to calculate error probabilities for other than linear receivers in impulsive noise. They include the effects of filtering the signal plus noise before detection. However, they do not include the effects of Gaussian noise. They also assume that only one noise impulse per signalling interval can occur and that the signalling interval can be broken up into signal-controlled and noise-controlled intervals.

With this survey complete, a more detailed statement of the problem considered in this thesis will be given.

III. STATEMENT OF THE PROBLEM

Consider the block diagram shown in Figure 1 of a general, coherent, binary communications system. The wideband filter, characterized in the time domain by its impulse response g(t), represents bandlimiting by the channel through which the binary signal passes. This filter will be called the radio frequency (rf) filter. The nonlinear block, to be discussed in more detail shortly, is chosen to suppress the detrimental effects of the impulse noise. The matched filter, which has impulse response h(t), is matched to s(t) which may be the difference of two binary signals. The noise, n(t), is considered to be an additive combination of white Gaussian noise and white impulsive noise.

The problem considered in this thesis is the determination of a good nonlinear device, such that the probability of error is minimized. As a consequence of finding this roughly "optimum" nonlinear device the probability of error for the system will also be obtained.

A closer look at the communication system model will be helpful in understanding the problem. In Figure 1 the matched filter block, along with the sampler and the threshold device, is the optimum receiver (optimum meaning minimum probability of error) for detection of a known signal embedded in additive, white Gaussian noise. (See [7] or [8]) A filter matched to the signal s(t), $0 \leq t \leq T_o$, has impulse response

$$h(t) = \begin{cases} S(T_o - t), & 0 \leq t \leq T_o \\ 0, & \text{otherwise.} \end{cases} \tag{3-1}$$

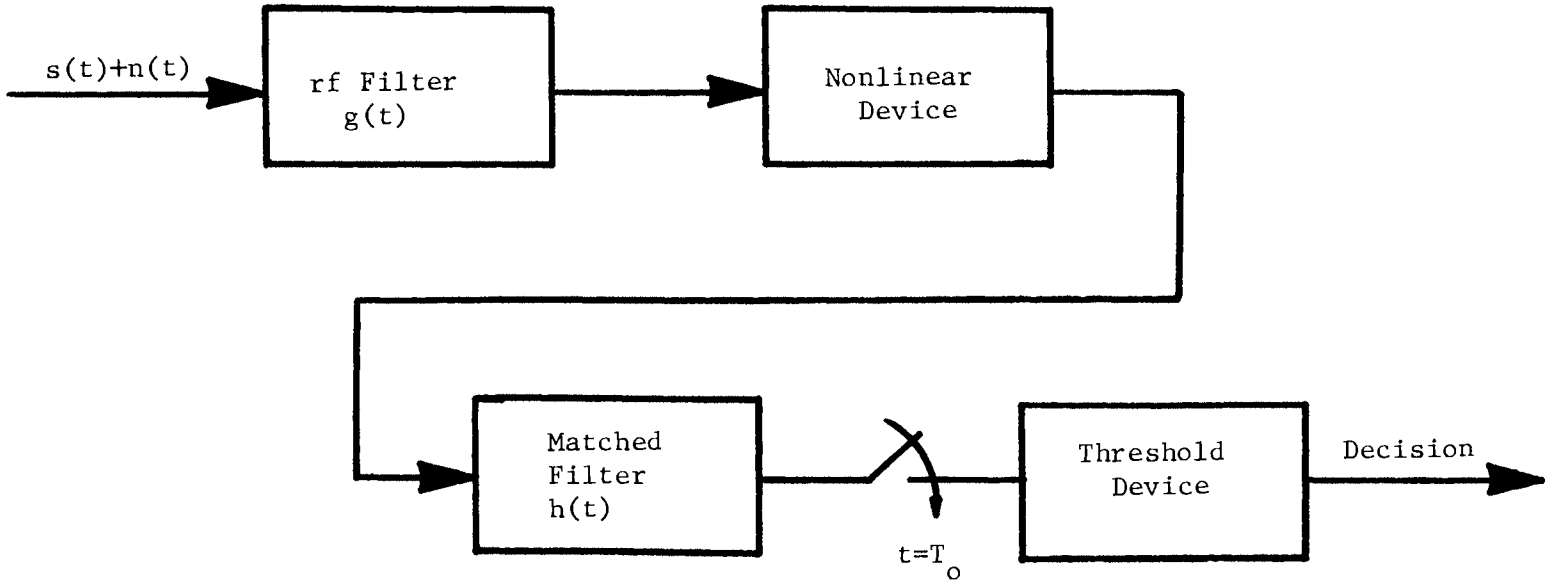

Figure 1.

Coherent Binary Communications System

For the general binary case, in which the detector is to decide which of two signals, $S_o(t)$ or $S_1(t)$, has been sent, it follows that the optimum receiver can base its decision on the difference, $S_o(t)-S_1(t)$, between the two signals. (See [8], pp. 254-257). That is, the filter can be matched to the difference of the signals. See Figure 2.

There is a particularly simple way to implement the watched filter in this receiver. Since the output of the matched filter is sampled only at the end of the signaling interval, $t=T_o$, any configuration that has the same output as the matched filter at $t=T_o$ is an acceptable implementation. If x(t) and y(t) are, respectively, the input and the output of a fixed, linear filter with impulse response h(t), then

$$y(t) = \int_o^t x(\tau)\, h(t-\tau)d\tau \quad . \tag{3-2}$$

But, for a filter matched to s(t),

$$h(t) = s(T_o-t), \quad 0 \leq t \leq T_o, \tag{3-3}$$

so,

$$y(t) = \int_o^t x(\tau)\, s(T_o-t+\tau)d\tau \quad . \tag{3-4}$$

Letting $t=T_o$ yields:

$$y(T_o)= \int_o^{T_o} x(\tau)\, s(\tau)\, d\tau \quad . \tag{3-5}$$

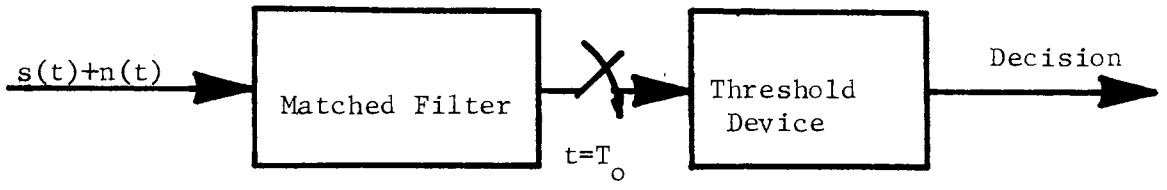

$$h(t) = \begin{cases} s_o(T_o-t)-s_1(T_o-t), & 0 \leq t \leq T_o \\ 0, & \text{elsewhere} \end{cases}$$

$$s(t) = \begin{cases} s_o(t) \\ s_1(t) \end{cases}$$

$n(t)$ is white Gaussian noise.

Figure 2.

Optimum Receiver for Binary Signal Detection in White Gaussian Noise.

Thus, if x(t) is multiplied by s(t) and the resulting function integrated from t=0 to $t=T_o$, a perfectly good implementation of the matched filter results. Such an implementation is called a correlation detector. Note that s(t) can be the difference of two signals.

Now, consider a noise process, $n_I(t)$, which will be called impulsive, or impulse, noise. The model used here will be similar to that used by Middleton [9], pp. 490-506.

$$n_I(t) = \sum_i a_i \, \delta(t-t_i) \tag{3-6}$$

where the a_i's are random variables with identical probability density functions (pdf's) which are symmetric about zero, δ is the Dirac-delta function, and the t_i's are random variables such that the number of impulses in the signaling interval, $[0, T_o]$ has a Poisson distribution. That is;

$$P_{T_o}(k) = \frac{(fT_o)^k}{k!} \exp\,[-(fT_o)], \tag{3-7}$$

$$k = 0,1,2,\ldots$$

where $P_{T_o}(k)$ is the probability that exactly k impulses occur in the interval t=0 to $t=T_o$ seconds, f is the average number of impulses per second and therefore fT_o is the average number of impulses per signalling interval. We note that $n_I(t)$ is a white noise process since its power spectral density is a constant. (See [7], p. 46.)

If the input of a matched filter receiver (Figure 2) is s(t) + $n_I(t)$ it is no longer the optimum receiver for detection of s(t) since $n_I(t)$ is not white Gaussian noise. However, the use of a suitable

nonlinearity prior to the matched filter should improve the receiver performance in impulsive noise, as the discussion below will show.

Intuitively we can think of an impulse function as having infinite height and zero duration. The fact that an impulse has any energy at all derives from the fact that it has infinite height. If a nonlinear device is placed before the matched filter as in Figure 3, and if the nonlinear device is such that it limits the maximum output to a finite value, the energy of the impulse noise will be reduced to zero. Hence, the effects of the impulse noise will be eliminated entirely.

What the above discussion points out, however, is not a perfect solution to the problem of impulsive noise, but a breakdown of the model itself. Ideal impulses do not exist in actual physical systems, and in communication systems impulse noise consists of pulses with finite height and non-zero duration. Also, the problem is complicated by the fact that Gaussian noise is normally present also and the presence of a nonlinear device makes the system sub-optimum for Gaussian noise. By adding the rf filter the problem is made more realistic. If we let $n(t) = n_I(t) + n_{WG}(t)$, where $n_{WG}(t)$ is white Gaussian noise and $n_I(t)$ is as defined by Equation (3-6), the output of the rf filter will be the sum of the filtered version of $s(t)$, the filtered version of $n_I(t)$, and the filtered version of $n_{WG}(t)$. The problem is then to find the "optimum" nonlinear device for this system.

It is desirable, of course, to obtain an analytic solution to this problem, but such a solution is difficult to find. In order to

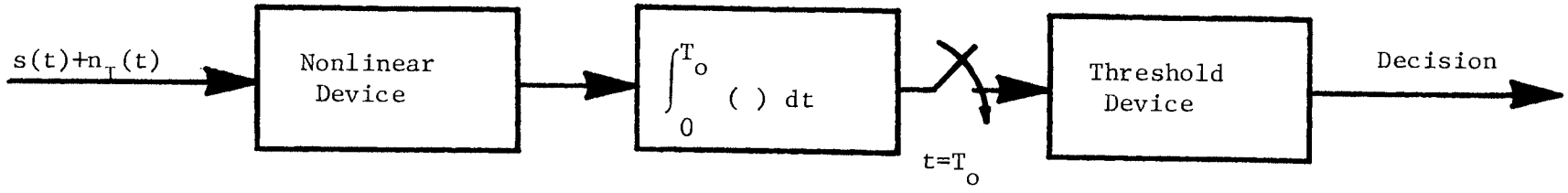

Figure 3.

Binary Communications System to Reduce
The Effects of Impulsive Noise

obtain an analytic solution, the pdf of the output of the matched filter at time $t=T_o$ is required. From this an expression for the probability of error for the system can be obtained. With this, the optimum characteristic for the nonlinear device could, in principle, be found by minimizing the probability of error with respect to the parameters of the nonlinearity. In order to do this, the type of nonlinearity considered would probably have to be restricted to certain classes, since the number of variable parameters would have to be relatively small.

The main problem with this method is obtaining the necessary pdf. The complication of the nonlinear device, along with the non-Gaussian nature of the noise, makes the mathematics virtually impossible.

In the absence of a clear route to follow to obtain an analytic solution, computer simulation appeared to be the best alternative. A Fortran program simulation of the system was written in which the Monte Carlo method of approximating the probability of an event by its relative frequency was used. The ratio of the number of errors to the total number of bits gives an estimate of the probability of error for the simulated communication system.

It would be desirable to simulate the system just as it is in Figure 1. If the PSK signal is:

$$S_{rf}(t) = \begin{cases} \sqrt{\frac{2E}{T_o}} \cos w_o t, & \text{for a binary 0} \\ \sqrt{\frac{2E}{T_o}} \cos (w_o t + \pi) & \text{for a binary 1} \end{cases} \qquad (3\text{-}8)$$

$$\text{for } 0 \leq t \leq T_o$$

depending on which binary message was sent, where E is the total energy of the signal, T_o is the signaling interval duration in seconds, and w_o is the carrier frequency in radians per second, it is seen that, normally, the signal contains high frequency components. This is obviously difficult to simulate because of the high sampling rate required, thereby resulting in an inordinate amount of computer time. It is more practical to do the simulation at baseband; that is, the input data to the receiver is translated to zero frequency, or baseband.

As will be shown, it is a simple matter to translate the linear portion of the system of Figure 1 to baseband. However, this translation cannot be done for the nonlinear device. This made it necessary to use a model such as that shown in Figure 4. In this system, the received signal plus noise is first translated to baseband, the nonlinear operation is then carried out, and the signal is detected by the matched filter and the threshold device.

Of course, baseband limiting places restrictions on the type of system which can be simulated. Any system which does its limiting at radio frequency (r.f.) could not be simulated by this method. An example is the system of Figure 1. However, there are practical phase reference devices which employ nonlinearities at baseband frequencies and the simulation carried out here would typify such systems.

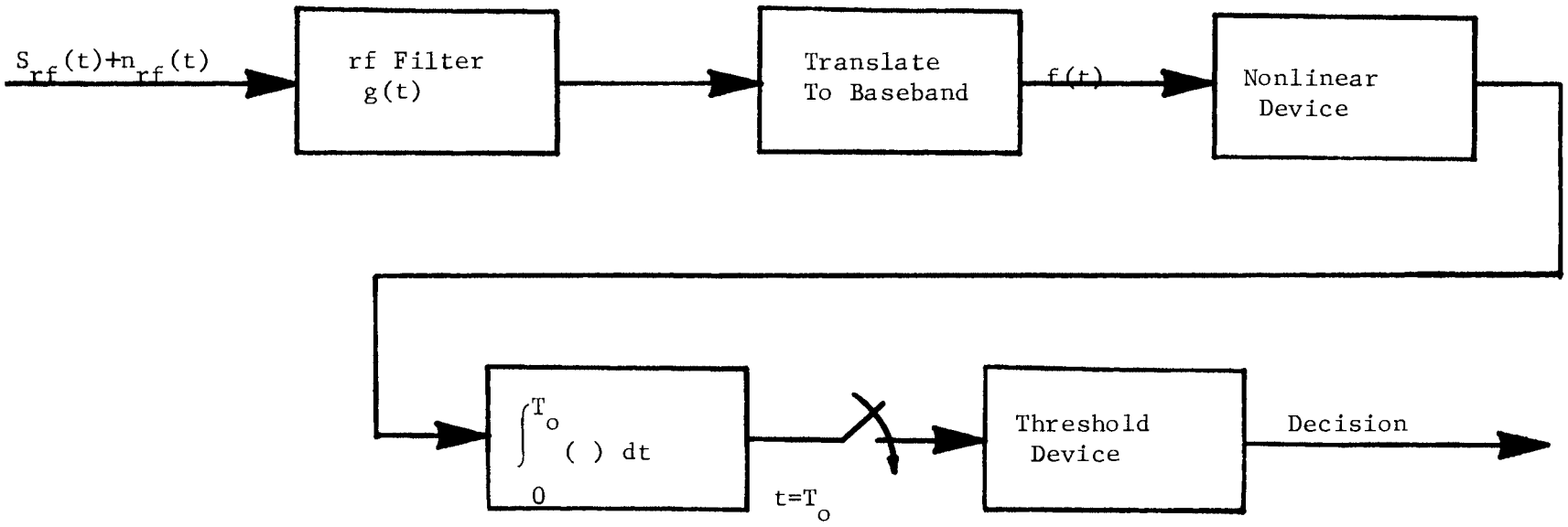

Figure 4

System Simulated

IV. SYSTEM SIMULATION

The block diagram of Figure 4 represents the system simulated. The binary PSK signals, as given by Eq. (3-8) are assumed to be a priori equally likely. Intersymbol interference was not considered, and since the pdf of the noise is assumed to be symmetric about zero, the simulation can be done using only one signal without loss of generality. In this simulation $S_{rf}(t) = \sqrt{\frac{2E}{T_o}} \cos w_o t$, $0 \leq t \leq T_o$ was chosen.

The noise is represented by $n_{rf}(t) = n_I(t) + n_{WG}(t)$ (4-1)

where $n_I(t)$ and $n_{WG}(t)$ are the previously discussed white impulsive noise and white Gaussian noise respectively.

Because the simulation is done at baseband, it is convenient to represent all signals in terms of complex envelopes. This representation will now be discussed. In general, a narrowband signal $S_{rf}(t)$ can be represented in terms of the envelope and phase functions by:

$$S_{rf}(t) = M(t) \cos[w_o t + \phi(t)] \tag{4-2}$$

where M(t) is the amplitude modulation and $\phi(t)$ is the phase modulation. (See [7], p. 12). The signal can also be represented in terms of the quadrature components of the signal:

$$S_{rf}(t) = X(t) \cos w_o t - Y(t) \sin w_o t \tag{4-3}$$

Noting that the PSK signal used here can be written as:

$$S_{rf}(t) = \pm \sqrt{\frac{2E}{T_o}} \cos w_o t \tag{4-4}$$

it follows that $\phi(t)=0$ and $M(t)=\pm\sqrt{\frac{2E}{T_o}}$. (4-5)

Also, $Y(t)=0$ and $X(t)=\pm\sqrt{\frac{2E}{T_o}}$

Since the positive signal was chosen for this simulation,

$$X(t)=+\sqrt{\frac{2E}{T_o}} \tag{4-6}$$

is used here.

The complex envelope, $F(t)$, of a signal is defined by:

$$F(t)=X(t)+jY(t)=M(t)\,e^{j\phi(t)}. \tag{4-7}$$

For the signal used, $F(t)=\sqrt{\frac{2E}{T_o}}$, which is real in this case. Note that $S_{rf}(t)$ can be expressed in the form:

$$S_{rf}(t)=\mathrm{Re}[F(t)e^{jw_o t}] \tag{4-8}$$

where Re[ ] means the real part of the argument. Given a linear filter with impulse response $g(t)$, input $S_{rf}(t)$ and output $S_o(t)$ (Figure 5), it can be shown that [7]:

$$S_o(t)=\mathrm{Re}[F_o(t)e^{jw_o t}] \tag{4-9}$$

where

$$F_o(t)=g_{bb}(t) * F(t). \tag{4-10}$$

The * indicates convolution, and $g_{bb}(t)$ is the complex envelope of the impulse response $g(t)$. In deriving Equation (4-10), the assumption is made that the magnitudes of the Fourier transforms of $S_o(t)$, $g(t)$, and $S_{rf}(t)$ are appreciable only in the neighborhood of w_o and zero elsewhere. That is $S_{rf}(t)$, and $g(t)$ are narrowband.

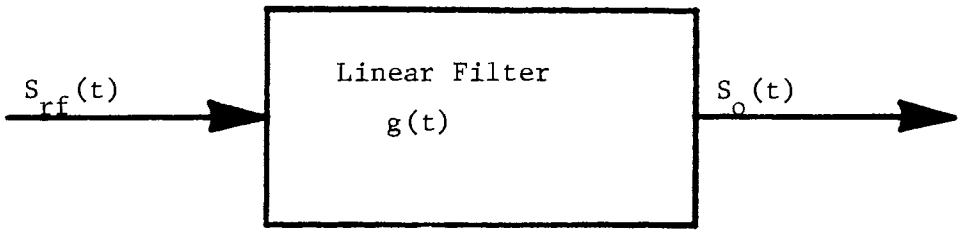

Figure 5.

Linear Filter with Impulse Response g(t).

The impulse response g(t) is given in terms of its complex envelope by:

$$g(t) = 2\mathrm{Re}[g_{bb}(t)\, e^{jw_o t}] \tag{4-11}$$

But if g(t) is the impulse response of a filter with a symmetric, narrowband transfer function, then $g_{bb}(t)$ is real [10]. In this case narrowband means that the passband of the rf filter is much smaller than the carrier frequency w_o. In the statement of the problem, the rf filter was referred to as a wideband filter. There is no inconsistency here because the rf filter is considered to have a relatively large bandwidth when compared with the bit rate bandwidth, $1/T_o$. These requirements are normally satisfied for practical systems.

Since $g_{bb}(t)$ is real, $F_o(t)$ is real and

$$S_o(t) = \mathrm{Re}\, F_o(t)\, e^{jw_o t} \tag{4-12}$$

$$S_o(t) = F_o(t)\, \mathrm{Re}\, e^{jw_o t} \tag{4-13}$$

$$S_o(t) = F_o(t) \cos w_o t \tag{4-14}$$

$$\text{Since } F_o(t) = g_{bb}(t) * F(t), \tag{4-10}$$

it is an easy matter to find $S_o(t)$.

To determine the response of the rf filter to the noise impulses, g(t) must be expressed in terms of the low frequency equivalent $g_{bb}(t)$.

$$g(t) = 2\, \mathrm{Re}[g_{bb}(t)\, e^{jw_o t}] \tag{4-11}$$

$$g(t-t_k) = 2\mathrm{Re}\ g_{bb}(t-t_k)\ e^{jw_o t}\ e^{-jw_o t_k} \tag{4-15}$$

$$g(t-t_k) = 2\ g_{bb}(t-t_k)[\cos w_o t_k \cos w_o t + \sin w_o t_k \sin w_o t] \tag{4-16}$$

To translate the noise impulse back to baseband, $g(t-t_k)$ is multiplied by the $\cos w_o t$ and the high frequency terms are filtered out.

$$\cos w_o t\ g(t-t_k) = 2g_{bb}(t-t_k)[\cos^2 w_o t \cos w_o t_k + \cos w_o t \sin w_o t \sin w_o t_k] \tag{4-17}$$

$$= 2g_{bb}(t-t_k)[1/2 + 1/2 \cos 2w_o t) \cos w_o t_k + 1/2 \sin 2w_o t_k \sin w_o t_k] \tag{4-18}$$

Filtering out high frequency terms, a noise impulse translated to baseband is:

$$g_{bb}(t-t_k) \cos w_o t_k, \quad t \geq t_k. \tag{4-19}$$

Let the filtered impulsive noise be denoted by $n_{fI}(t)$:

$$n_{fI}(t) = \sum_k a_k\ g_{bb}(t-t_k) \cos w_o t_k \tag{4-20}$$

Note that $g_{bb}(t-t_k)=0$ for $t < t_k$.

The next component which must be calculated is the output of $g_{bb}(t)$ due to the white Gaussian noise, which will be a colored Gaussian noise process. To simulate the Gaussian noise a first-order Markov approximation was used. This approximation was obtained from the second-order pdf for the process as follows ([7], p. 54): Let

n_1 and n_2 be random variables representing the possible realizations of a Gaussian noise process, n(t), at times t_1 and t_2 respectively, where $t_2 > t_1$. Assuming a stationary, zero-mean process, the second-order pdf $p_2(n_1,n_2)$ is bivariate normal:

$$p_2(n_1,n_2) = \frac{1}{2\pi\sigma^2\sqrt{1-\rho^2}} \exp\left[-\frac{n_1^2-2\rho n_1 n_2+n_2^2}{2\sigma^2(1-\rho^2)}\right] \qquad (4\text{-}21)$$

where

$\sigma^2 = \mathrm{Var}(n) =$ variance of n.

$$\rho = \frac{\phi_o(t_2-t_1)}{\phi_o(0)}$$

$\phi_o(\tau)$ is the autocovariance function of $n(\tau)$ defined as

$$\phi_o(\tau) = E\{(n(t)-E[n(t)])(n(t+\tau)-E[n(t+\tau)]\} \qquad (4\text{-}22)$$

where E[·] means the expected value of the argument. Note that $\phi_o(\tau)$ can be obtained from the inverse Fourier transform of $\Phi_o(w)$, the power spectral density. (See Figure 6).

The conditional p.d.f. of n_2 given n_1, $p_1(n_2 \mid n_1)$, is:

$$p_1(n_2 \mid n_1) = \frac{p_2(n_1,n_2)}{p(n_1)} \quad . \qquad (4\text{-}22)$$

The p.d.f. $p(n_1)$ is also Gaussian with variance τ^2 and mean zero. Performing the indicated division:

$$p_2(n_2 \mid n_1) = \frac{1}{\sqrt{2\pi\sigma^2(1-\rho^2)}} \exp\left[-\frac{(n_2-\rho n_1)^2}{2\sigma^2(1-\rho^2)}\right] \qquad (4\text{-}24)$$

This p.d.f. is also Gaussian with the following mean and variance:

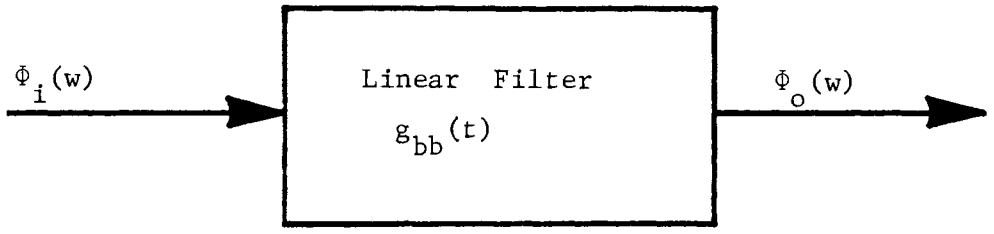

$$\Phi_o(w) = |G_{bb}(w)|^2 \Phi_i(w)$$

$\Phi_i(w)$ is the power spectral density of the input noise process.

$\Phi_o(w)$ is the power spectral density of the output noise process.

Figure 6

Output Power Spectral Density From
The Input Power Spectral Density.

$$E[N_2 \mid n_1] = \frac{\phi_o(t_2-t_1)n_1}{\phi_o(0)} \tag{4-25}$$

$$Var[N_2 \mid n_1] = \sigma^2 \left[1- \left\{\frac{\phi_o(t_2-t_1)}{\phi_o(0)}\right\}^2\right]. \tag{4-26}$$

Given the autocovariance function, $\phi_o(\tau)$, and the value of a noise sample at t_1, n_1, the value for a noise sample at t_2, n_2, can be approximated by drawing a value from a Gaussian population with the above mean and variance. This method is only approximate, as was mentioned, since only a second-order density function was used. Actually, the noise sample at any one time would depend on all past values of the noise. However, the most recent value is the dominant value, so the second order approximation should give a reasonable estimate of colored Gaussian noise.

It is difficult to say anything quantitative about this approximation. However, since the autocovariance function of the noise falls off exponentially with time for the rf filter considered it seems likely that the most recent noise sample will have a much larger effect on the current noise sample than the next most recent sample.

Because the rf filter is a linear filter, its response to the sum of a number of components is the sum of the responses of each of the components. Therefore, the signal plus noise, translated to baseband and denoted by f(t), is

$$f(t)=1/2\ F_o(t)+ \sum_k a_k\ g_{bb}(t-t_k)\ \cos(w_o t_k)+ n_G(t), \tag{4-27}$$

where: $g_{bb}(t)$ is the low frequency impulse response of g(t).

$F_o(t) = g_{bb}(t) * F(t)$, which is the low frequency equivalent of the filtered signal.

$n_G(t)$ is colored Gaussian noise.

The time function f(t), indicated on the block diagram in Figure 4, is passed through the limiter and is then cross-correlated with the original baseband signal (i.e. the unfiltered baseband signal). It should be noted that this correlation detector, even without the non-linearity, is not the optimum detector for the filtered signal in colored Gaussian noise. However, since the rf filter is a relatively wideband filter, it is a reasonable approximation of the optimum system. This approximation is often used in practical receivers of this kind.

The output of the cross-correlator is compared with a threshold (the threshold is zero in the case of equally-probable, antipodal signals) and a decision is made as to which of the binary messages has been received.

The computer program for this simulation is included in Appendix A, along with a brief explanation of how it works.

V. RESULTS

For the results of the simulation presented here, $g_{bb}(t)$ was assumed to be the impulse response of a first-order Butterworth filter. Two bandwidths were chosen: $\frac{10}{\pi}$ x (Bit rate bandwidth) and $\frac{5}{\pi}$ x (Bit rate bandwidth). Recall that bit rate bandwidth is $\frac{1}{T_o}$.

The average number of impulses per bit period, fT_o, was 10^{-1}. The random impulse amplitudes, a_i's were selected from a zero-mean, Gaussian population.

The Monte Carlo method for computing probabilities is quite time consuming. Several things were done to conserve computer time. First, only a small set of possible non-linearities were considered. These are shown in Figure 7. In Figure 7, x and y are respectively the input and the output of each nonlinearity.

When the simulation is done without Gaussian noise, only a little more than one in every 10 bits, on the average, is perturbed by the presence of an impulse if $fT_o = 1/10$. (The average is more than one out of ten because a noise impulse may carry over into the next bit period.) Therefore, the unaffected bits can be assumed correct without running the entire simulation for these bits, and this was incorporated into the simulation.

The four limiters in Figure 7 were tested with the wider bandwidth of filter at a signal-to-noise-ratio (SNR) of -21.9 dB in order to get enough errors to give relative frequencies which closely approximate the error probabilities. The results were as follows:

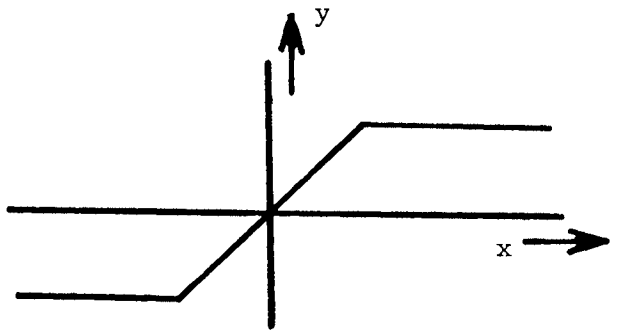

a. Limiter 1.

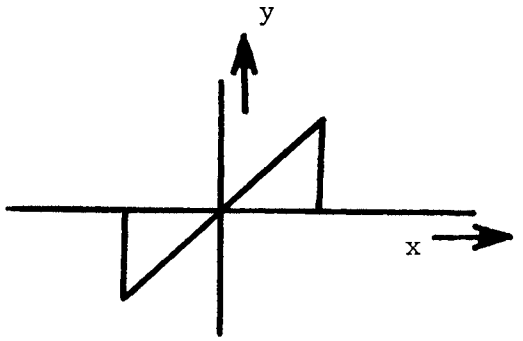

b. Limiter 2.

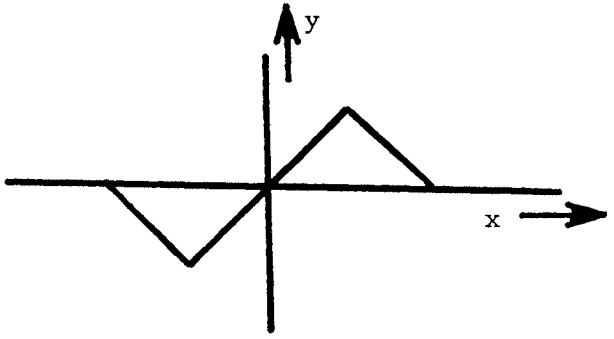

c. Limiter 3.

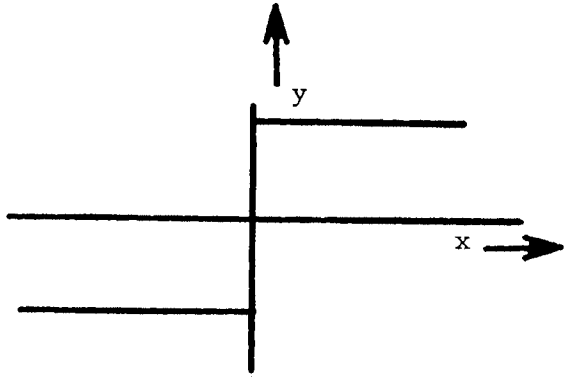

d. Limiter 4.

Figure 7.

Limiters Tested With Impulsive Noise Only

Limiter 1, probability of error = 0.033

Limiter 2, probability of error = 0.001

Limiter 3, probability of error = 0.003

Limiter 4, probability of error = 0.027

Clearly, limiters 2 and 3 are by far superior to the others. It was decided to choose limiter number 2 since it is the simpler of the two superior limiters. The difference in their probabilities of error was caused by only two errors in one thousand which is not a very significant difference.

The procedure, then, was to use limiter number 2 for Gaussian and impulsive noise together. Figure 8 shows limiter number 2 in more detail. The parameter P, measured in multiples of the signal amplitude, was varied in the simulation to obtain an optimum value of P.

Obviously a nonlinearity obtained in this manner is not truly optimum, and it may not even be the best among the four limiters considered for impulsive and Gaussian noise. But intuitively it should give a reasonable estimate of the optimum limiter. In any event, the problem of varying the parameters for all four limiters would be very time consuming, and, since limiters 1 and 4 were clearly inferior for impulse noise alone, it did not seem worth the extra computer time to carry out simulations on all four.

The results of the simulation are displayed graphically in Figures 9-20. Conditions for the simulations are summarized in Table I. The following terms are used in the discussion or on the graphs:

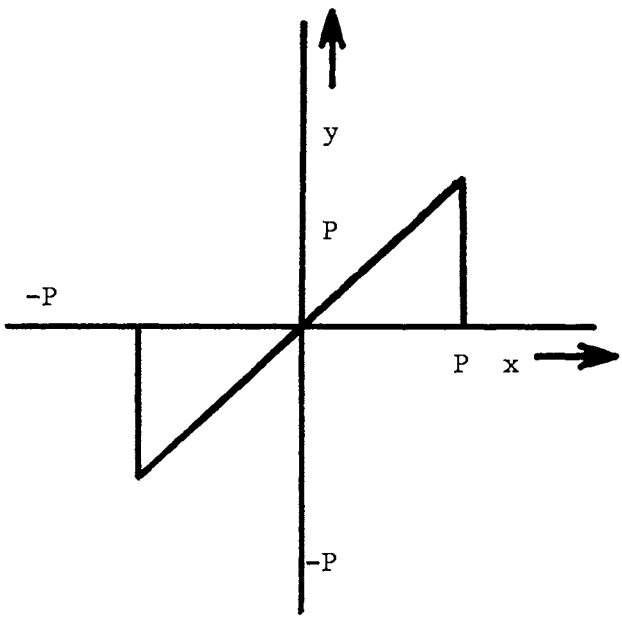

Figure 8.

Limiter Used For Additive Combination
of Gaussian and Impulsive Noise.

$$(1)\ \text{SNR} \triangleq 10 \log_{10}\left[\frac{E/T_o}{(\text{PSD} + \sigma^2 f)/T_o}\right] \qquad (4\text{-}1)$$

$$= 10 \log_{10}\left[\frac{\text{Signal power}}{\text{Noise power in bit rate bandwidth}}\right]$$

where:

E is the total signal energy in joules.

PSD is the bilateral power spectral density of the original white Gaussian noise process in (watts/Hz.).

σ^2 is the variance of the amplitudes of the noise impulses.

f is the average number of noise impulses per second.

$$(2)\ \text{RATIO} = \frac{\sigma^2 f}{\text{PSD} + \sigma^2 f} = \frac{\text{Impulse noise power spectral density}}{\text{Total noise power spectral density}} \qquad (4\text{-}2)$$

$$= \frac{\text{Impulse noise power}}{\text{Total noise power}}$$

(3) $P_e(P)$ is the probability of error as a function of the parameter P, where P is shown in Figure 8.

Note that E = 1.0 joule for all the graphs shown.

TABLE I.

CONDITIONS FOR EACH SIMULATION

Case	Figure	SNR (dB)	BW (xBit Rate Bw)	PSD (watts/Hz.)	$\sigma^2 f$ (watts/Hz.)	Ratio	f (Hz.)
1	9	0.0	$10/\pi$	0.5	0.5	0.5	200
2	10	-10.0	$10/\pi$	4.99	0.5	0.5	200
3	11	-13.5	$10/\pi$	2.49	19.97	0.89	200
4	12	-20.0	$10/\pi$	0.5	100.0	0.995	200
5	13	1.6	$10/\pi$	0.0635	0.629	0.91	200
6	14	2.0	$10/\pi$	0.00635	0.629	0.99	200
7	15	5.0	$10/\pi$	0.1587	0.1587	0.5	200
8	16	-1.5	$10/\pi$	0.1287	1.27	0.91	200
9	17	-34.0	$10/\pi$	0.1287	2534	0.99995	200
10	18	-1.85	$5/\pi$	0.254	1.96	0.833	200
11	19	-34.0	$5/\pi$	0.254	2539	0.9999	200
12	20	-8.8	$5/\pi$	4.99	1.2704	0.17	200

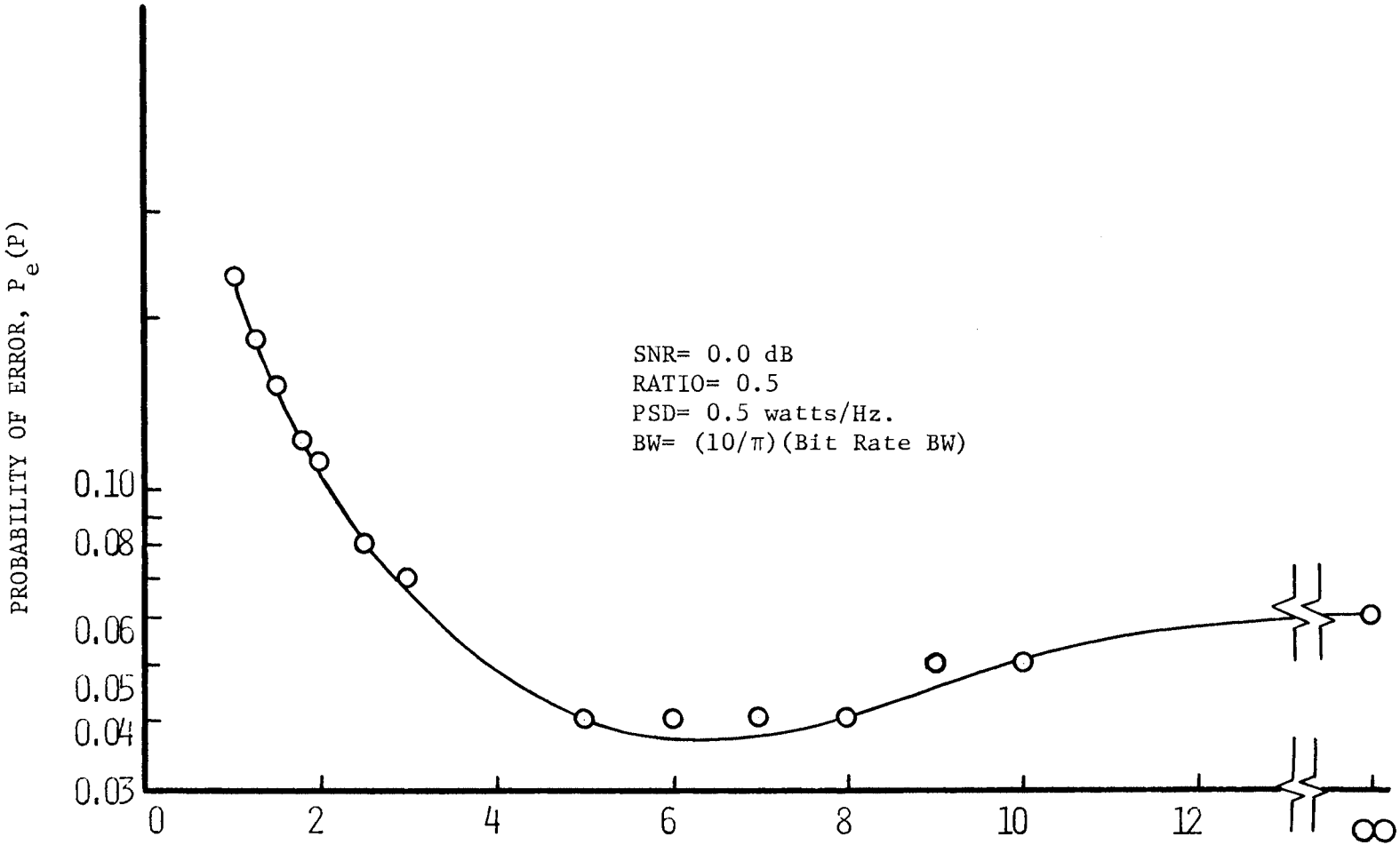

Figure 9. Probability of Error Versus Limiter Parameter Case 1

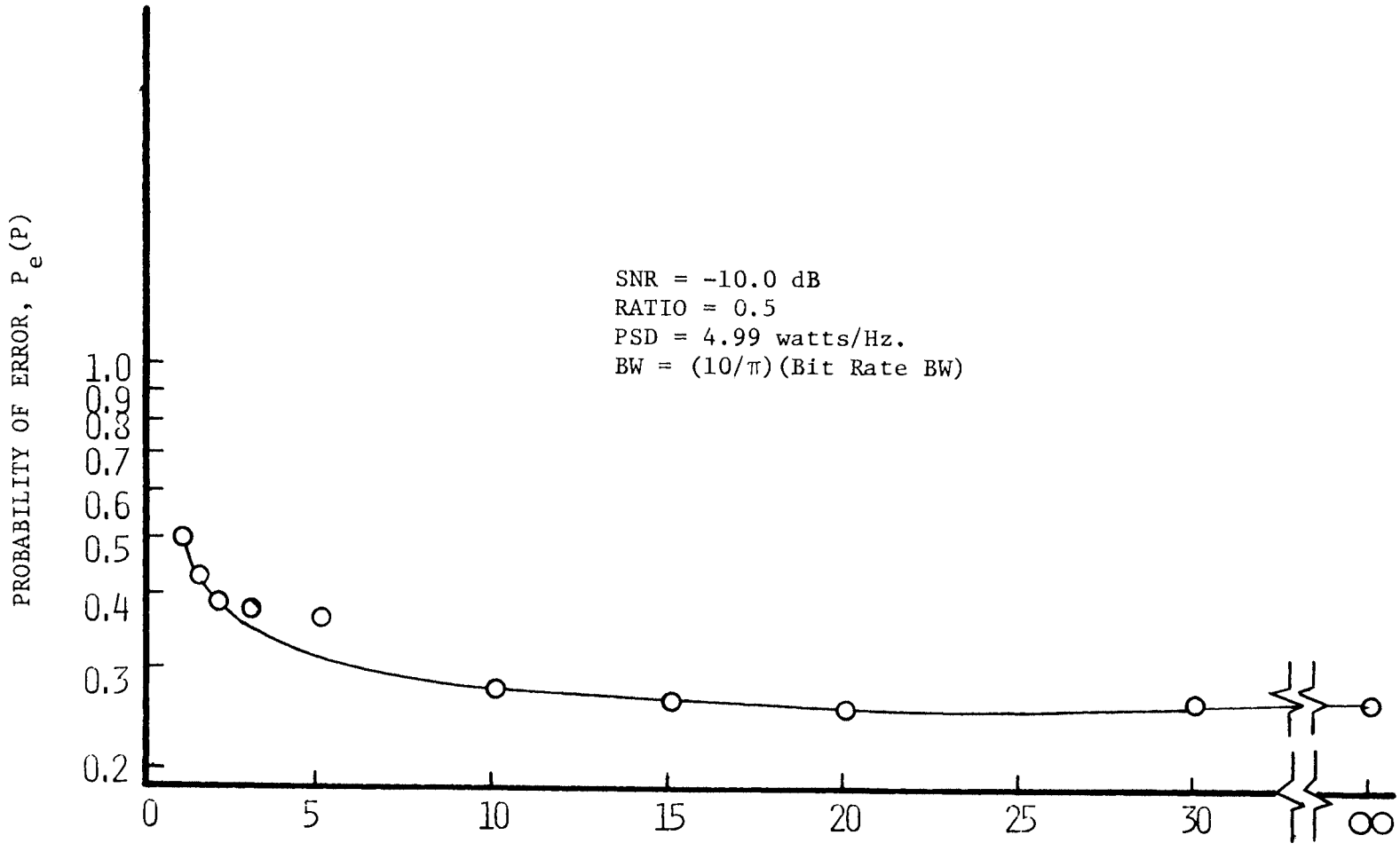

Figure 10. Probability of Error Versus Limiter Parameter Case 2

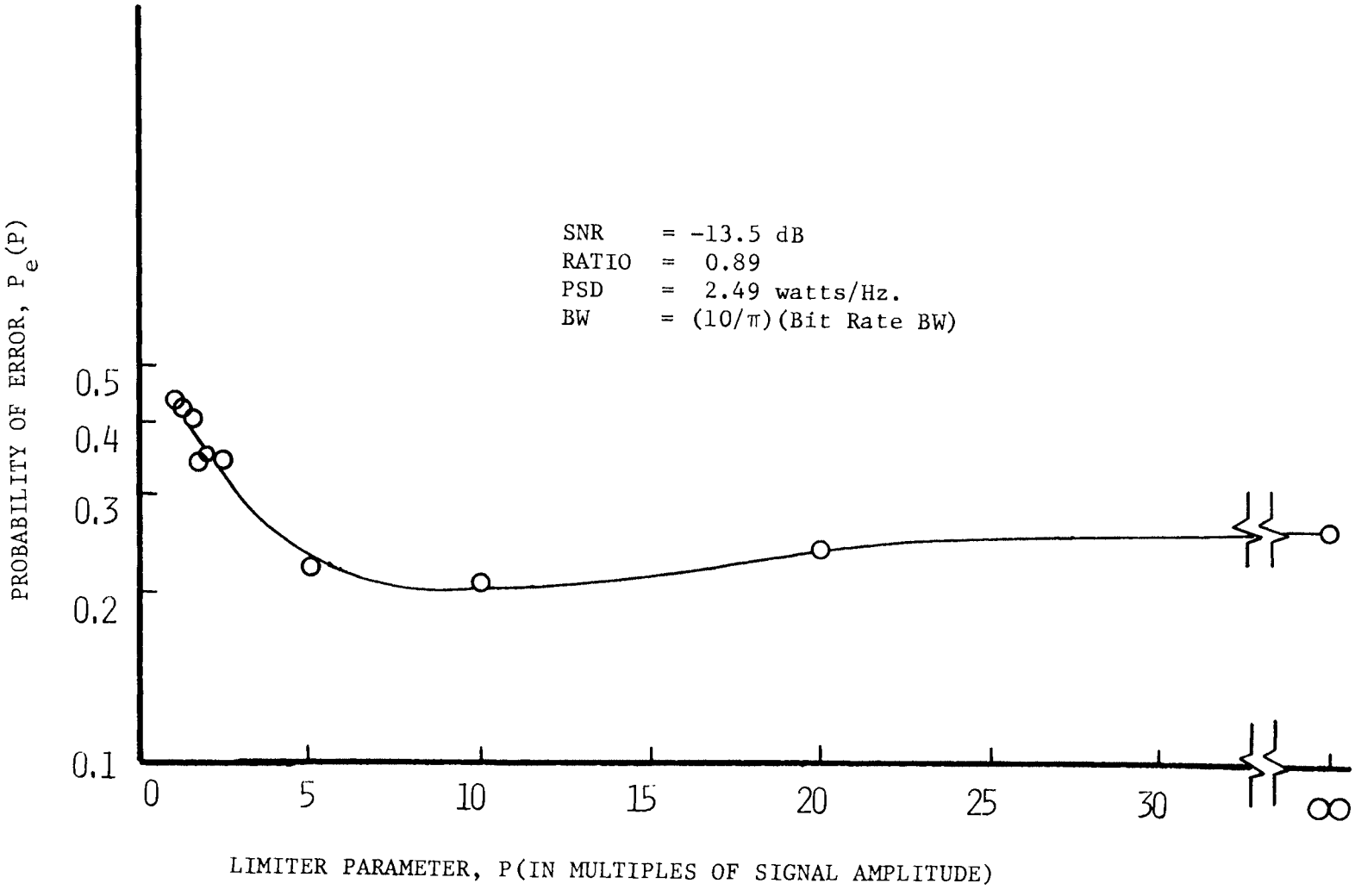

Figure 11. Probability of Error Versus Limiter Parameter Case 3

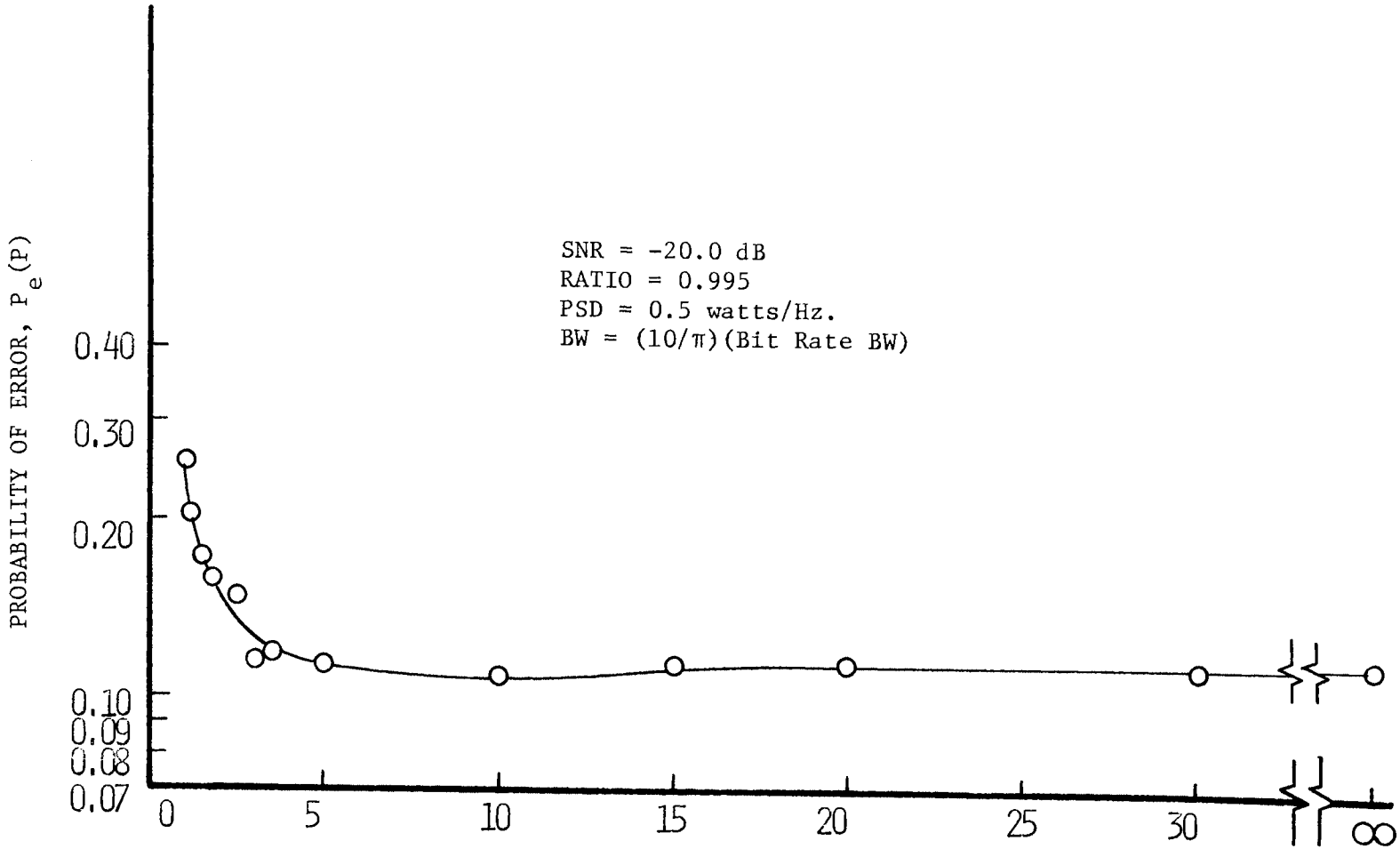

Figure 12. Probability of Error Versus Limiter Parameter Case 4

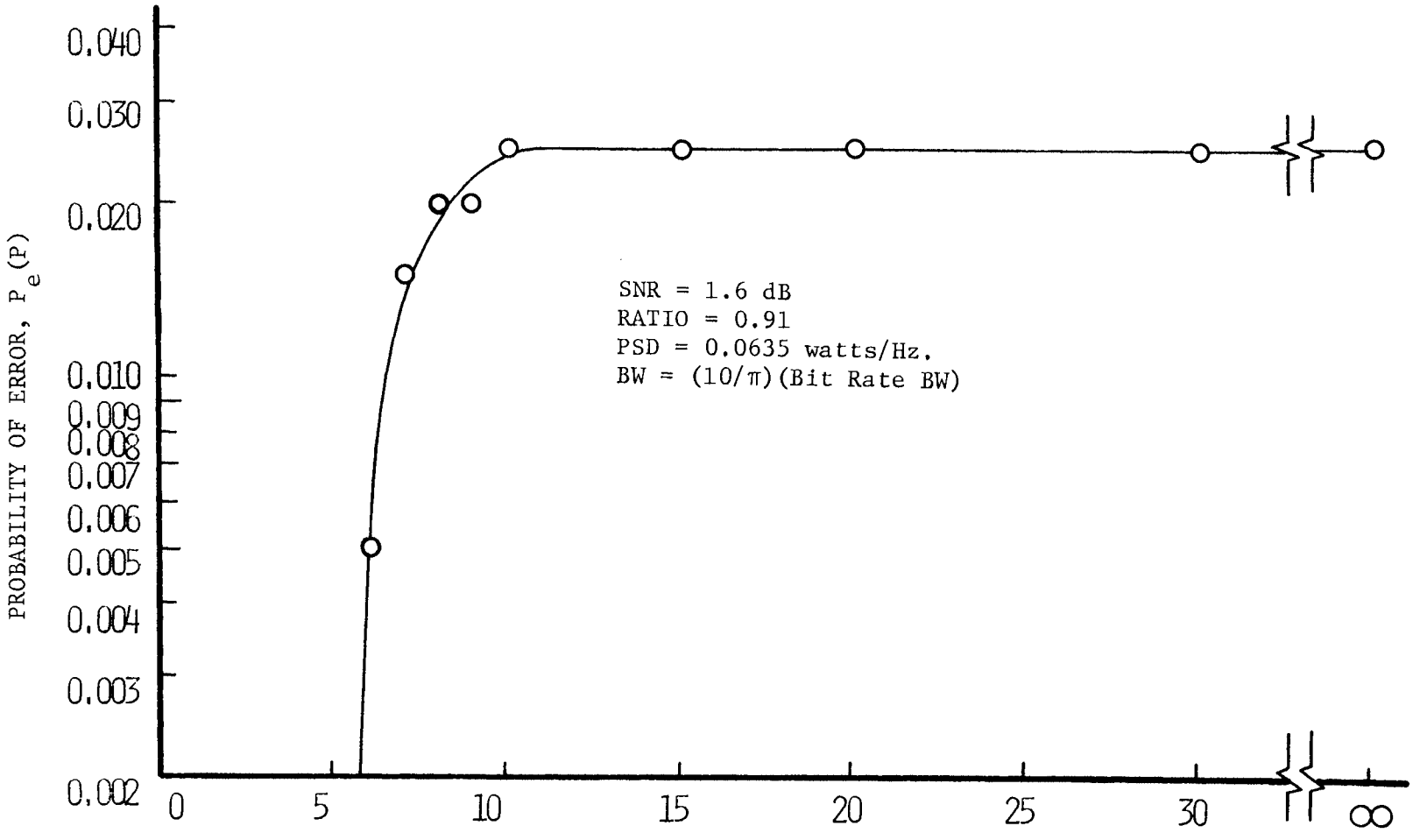

Figure 13. Probability of Error Versus Limiter Parameter Case 5

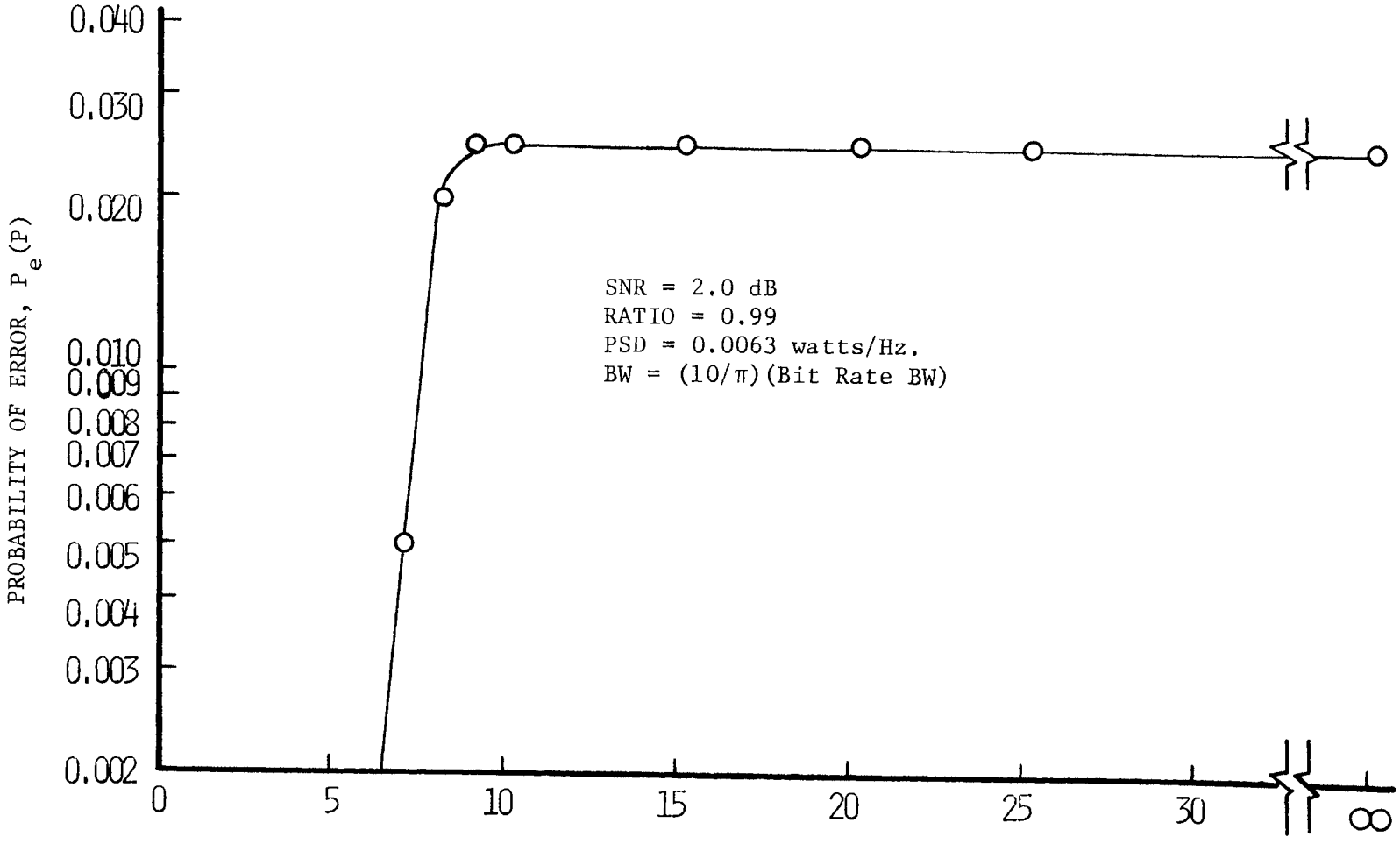

Figure 14. Probability of Error Versus Limiter Parameter Case 6

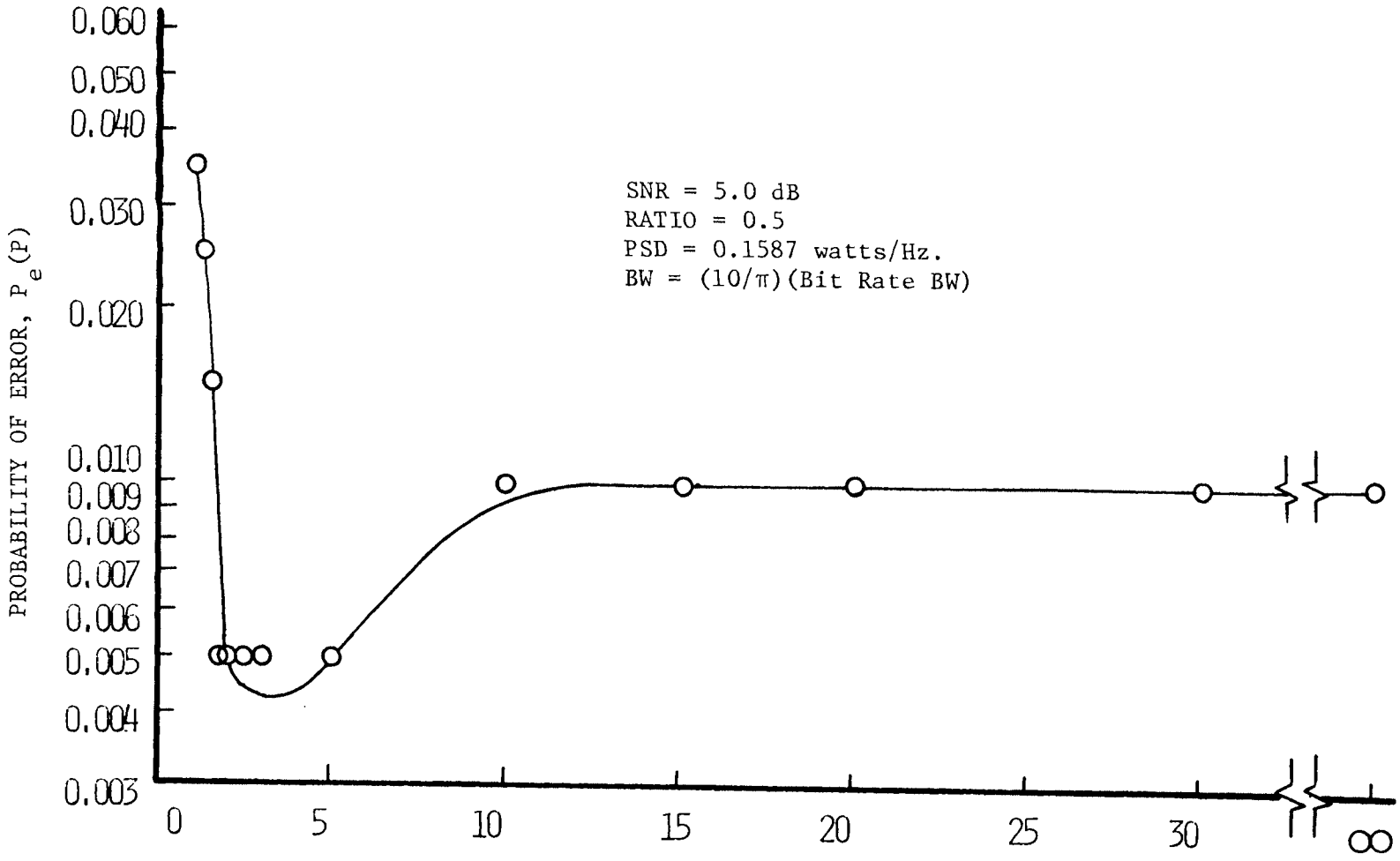

Figure 15. Probability of Error Versus Limiter Parameter Case 7

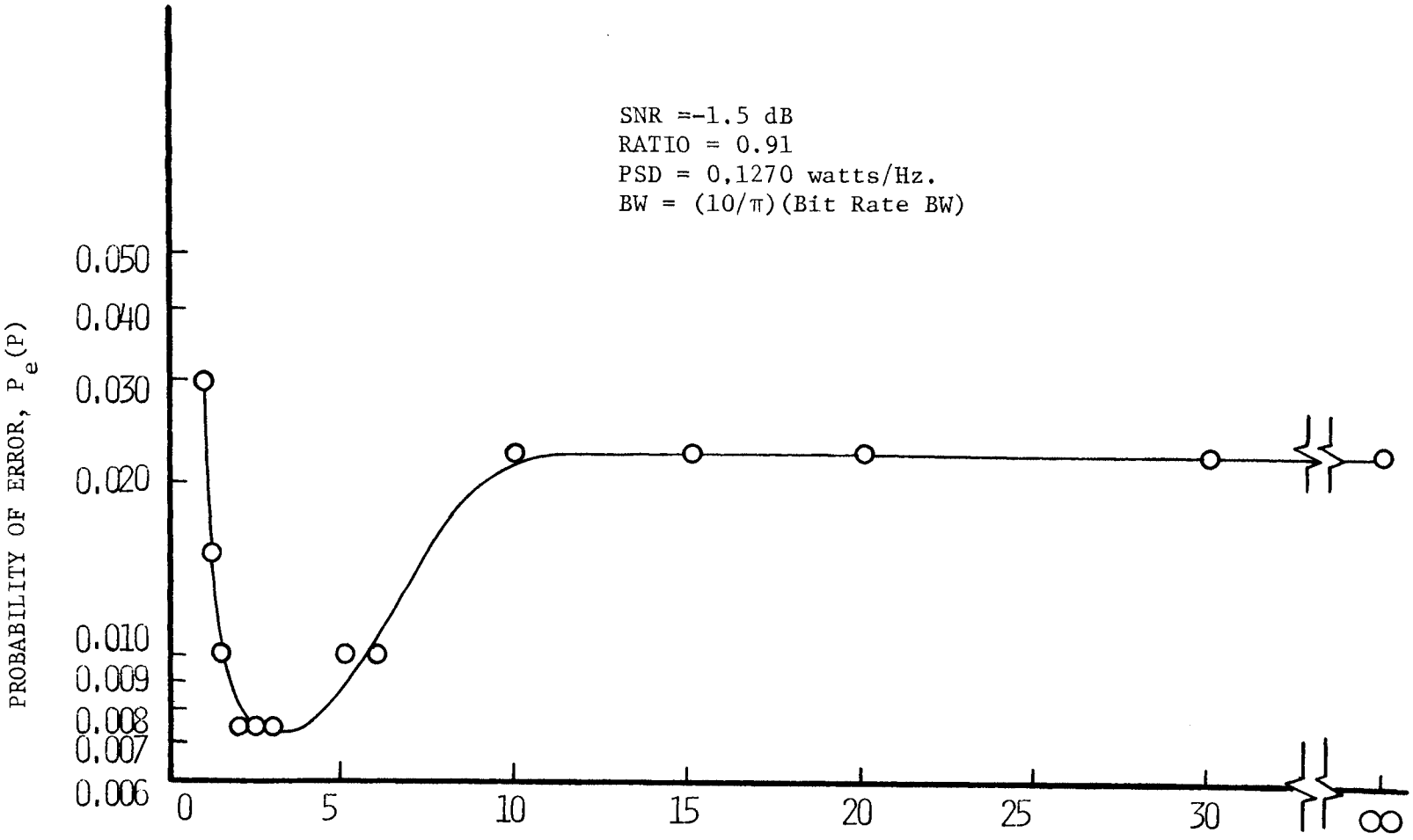

Figure 16. Probability of Error Versus Limiter Parameter Case 8

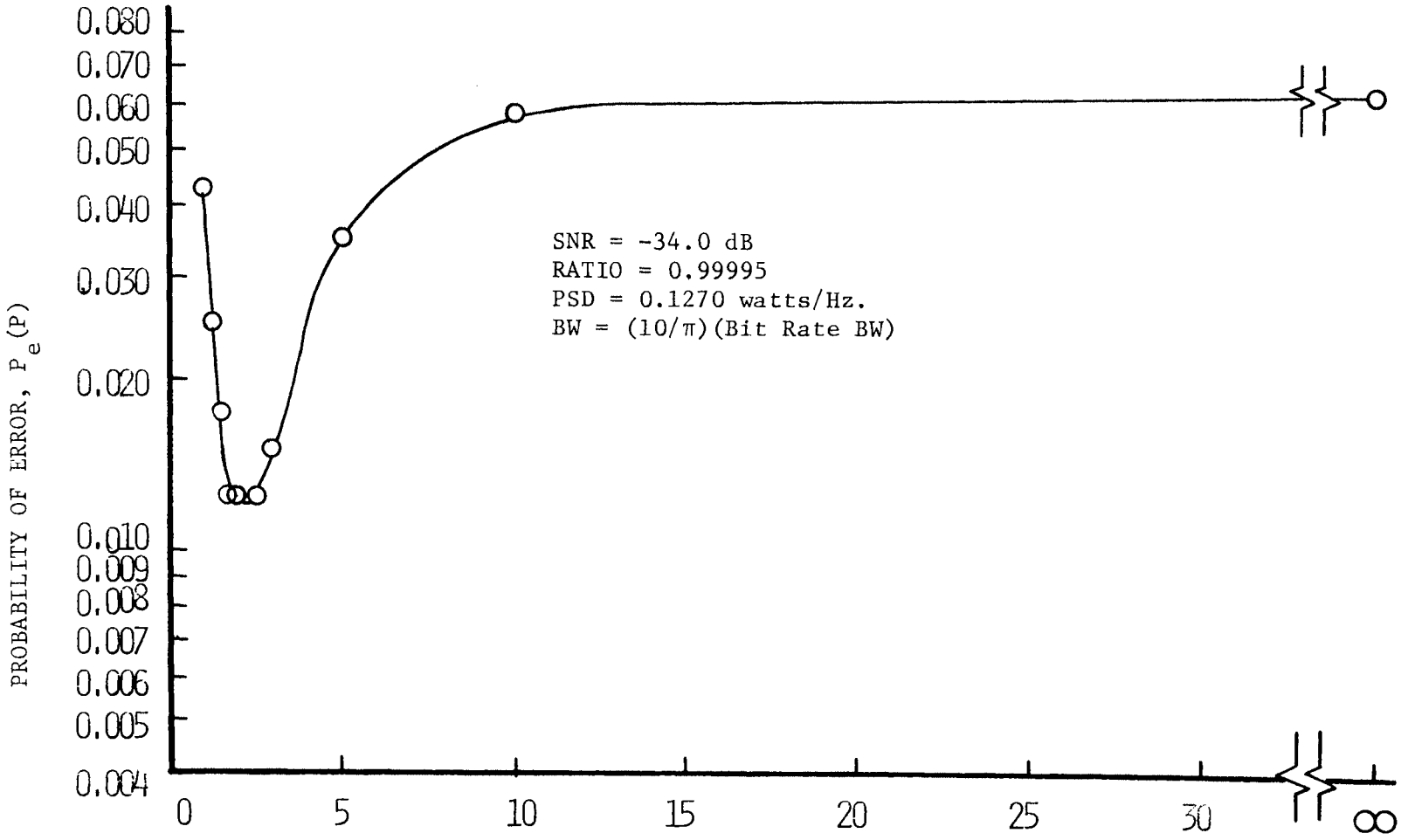

Figure 17. Probability of Error Versus Limiter Parameter Case 9

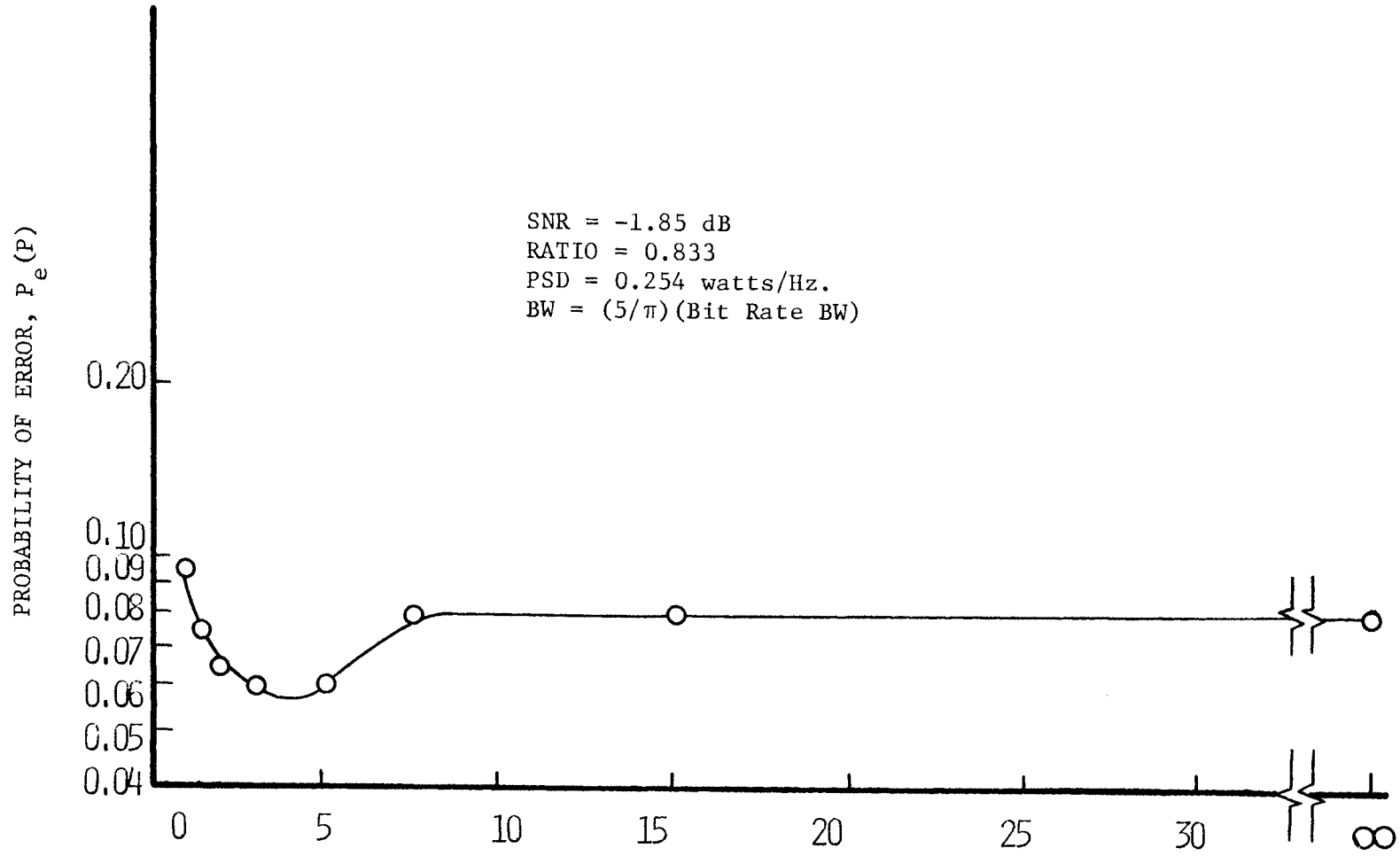

Figure 18. Probability of Error Versus Limiter Parameter Case 10

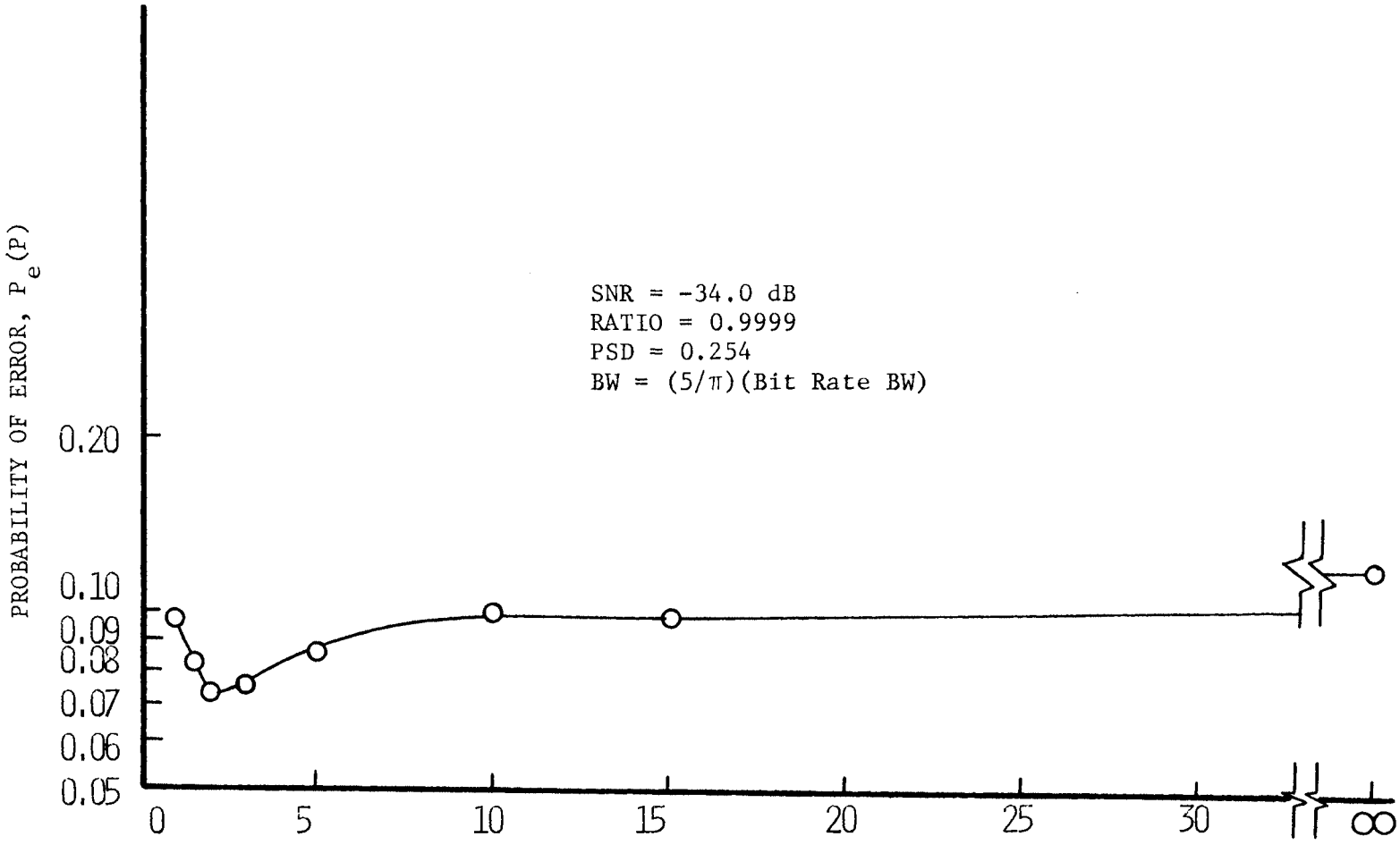

Figure 19. Probability of Error Versus Limiter Parameter Case 11

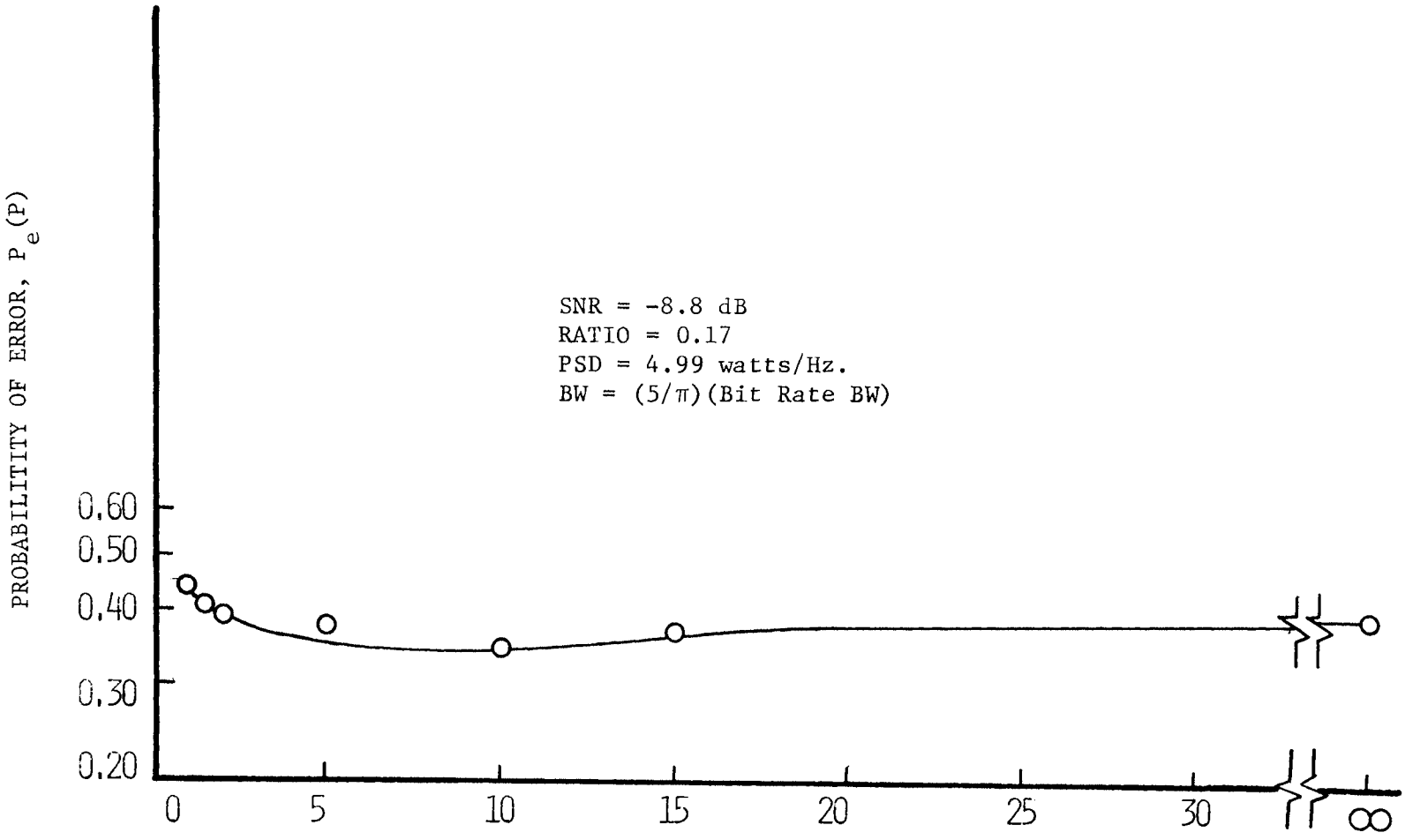

Figure 20. Probability of Error Versus Limiter Parameter Case 12

VI. DISCUSSION OF RESULTS

A brief look at Figures 9 through 20, shows that there are three general categories of graphs. They are:

1. $P_e(P)$ decreases and then increases as P increases, giving an optimum value or optimum range of values for the parameter P. For example see Figures 9, 11, 15-20.

2. $P_e(P)$ decreases and then levels off as P increases without attaining a minimum value or attaining only a very weak minimum. For example see Figures 10 and 12.

3. $P_e(P)$ increases and then levels off as P increases. Two examples are Figures 13 and 14.

Also note that on several of the graphs the curves flatten out or there are a few points which do not seem to fit the curve. This behavior is due to the simulation sample size being too small.

The three types of curves can be explained intuitively as follows:

1. For the curves included under category 1, the original decrease in $P_e(P)$ is caused by reducing the number of errors due to Gaussian noise. As P increases the system more nearly approaches the optimum (approximately optimum as explained earlier) receiver for Gaussian noise, which is the matched filter with no limiter (i.e. $P=\infty$). The increase in $P_e(P)$ as P increases further is caused by the impulsive noise as the limiting level is raised.

2. For the curves included in category 2, the original decrease in $P_e(P)$ is caused by the same mechanism as those in category 1. $P_e(P)$ does not increase or increases very slightly as P increases further

because the impulse noise power is not great enough to cause such an increase.

3. For the curves in category 3, the increase for higher values of P is caused by the same mechanism as for the graphs in category 1. (i.e. more errors are caused by impulsive noise as the limiting level is raised). However, in these graphs there were no errors indicated by the simulation for small values of P. This would indicate that the probability is quite small for P small. For P small, most errors are caused by Gaussian noise. It seems logical that these curves, too, would initially decrease as P increases if the probability of error had not been too small to estimate in this range, and that these graphs, also, would have an optimum value or optimum range of values for P. An extra 200 bits were simulated for small P but no errors were obtained again. For P small, most errors are caused by Gaussian noise. At this particular level of Gaussian noise power (Fig. 13), the probability of error for Gaussian noise only is less than 10^{-3}. So it is not surprising that out of 400 bits there were no errors.

An interesting comparison is the improvement obtained by using limiting with the optimum value of P as opposed to no limiting at all. This comparison is made in Table II, where R is the ratio of P_e at the optimum P to P_e at $P=\infty$.

Table II shows that the performance ratio improves, in most cases, with decreasing Gaussian noise power. This is reasonable because as the Gaussian noise power increases, the percentage of errors due to impulsive noise decreases and limiting does less for the system.

TABLE II

IMPROVEMENT DUE TO LIMITING

Figure	PSD $(\frac{\text{watts}}{\text{Hertz}})$	Ratio	Bandwidth (x Bit Rate BW)	R
9	0.5	0.5	$10/\pi$	0.67
10	4.99	0.5	$10/\pi$	0.96
11	2.49	0.89	$10/\pi$	0.81
12	0.5	0.995	$10/\pi$	0.96
13	0.0635	0.91	$10/\pi$	----
14	0.0063	0.99	$10/\pi$	----
15	0.1587	0.5	$10/\pi$	0.50
16	0.1270	0.91	$10/\pi$	0.33
17	0.1270	0.99995	$10/\pi$	0.20
18	0.254	0.833	$5/\pi$	0.73
19	0.254	0.9999	$5/\pi$	0.60
20	4.99	0.17	$5/\pi$	0.90

An interesting comparison can be made between Figures 16,17,18 and 19. The bandwidth of the rf filter in Figures 16 and 17 is twice that of Figures 18 and 19. The amount of Gaussian noise, however, is the same for both cases since the original spectral densities differ by a factor of two. The performance ratios are much better for the wider bandwidth rf filter system. In other words the limiter improves the performance of the wider bandwidth system much more than it improves the performance of the smaller bandwidth system. This is true because the energy of an impulse in the smaller bandwidth system is spread out more in time and less of the energy is clipped by a limiter. The fact that the pre-limiting bandwidth should be wide in the case of impulsive noise is well-known [11], p. 509.

Those graphs which exhibit an initial decrease in $P_e(P)$ as P increases will now be considered. In general, the greater PSD (the power spectral density of the original white Gaussian noise process) the greater P must be before the $P_e(P)$ curve levels off (that is, before the P_e curves reach a value within 4 or 5% of the minimum value). Therefore, the lower the Gaussian noise power, the lower the level of the limiting can be without seriously impairing the performance of the system.

Now consider the curves for the system with the larger bandwidth filter (Figures 9 through 17). The standard deviation of the Gaussian noise is proportional to $\sqrt{PSD}$. The standard deviation can be considered to be, in an intuitive sense, a measure of the r.m.s. amplitude of the Gaussian noise. By examining the curves, it is seen that the minimum point of $P_e(P)$ occurs at values of P

which range between 4 and 6 times the value of $\sqrt{PSD}$ above the level of the signal.

This is not to say that the amount of impulsive noise has no effect on the optimum value of P. This is illustrated by Figures 16 and 17. In both figures the level of the Gaussian noise is the same, but the amount of impulsive noise in Figure 17 is much greater than in Figure 16. In Figure 16 the optimum value of P is about 3.0. In Figure 17 the optimum P is about 2.0 to 2.5. This shows that an increase in impulsive noise does lower the optimum value of P. However, a drastic change in impulsive noise is required to yield this relatively small change in the optimum P.

Now consider Figures 18 through 20, which are for the smaller bandwidth channel, BW=$(5/\pi)$(Bit Rate BW), where BW means bandwidth. The results for this bandwidth are similar to the larger bandwidth case. For Figures 18 and 20 the minimum occurs at about 6 and 4.6 times the $\sqrt{PSD}$, respectively, above the magnitude of the signal. These two values are near the values obtained for the wide bandwidth case. However, the power of the noise at the smaller bandwidth is one-half the power of the noise at the larger bandwidth for the same PSD, since the bandwidths differ by a factor of two.

If we consider a bandwidth factor, BWF, where BWF=1 for the $10/\pi$(Bit Rate BW) system, and BWF= 1/2 for the $5/\pi$(Bit Rate BW) system, then (PSD)(BWF) is proportional to Gaussian noise power for either bandwidth. For the larger bandwidth system the minimum point would still occur at between 4 and 6 times $\sqrt{(PSD)(BWF)}$.

But for the $5/\pi$(Bit Rate BW) system, Figures 18 and 20 would have their minimums occurring at 8.5 and 6.4 times $\sqrt{(PSD)(BWF)}$, respectively, above the signal level. It is difficult to say why this difference exists between the two systems with different bandwidth rf filters. The noise impulses in the smaller bandwidth case are, of course, smaller in amplitude but are more spread out than in the larger bandwidth case. Another factor which may enter in is that the smaller the bandwidth of the rf filter, the "less optimum" the matched filter system becomes.

The above factors do not seem to indicate why the optimum limiting level is higher for the smaller bandwidth system. Another factor is that the number of simulations and the number of samples may be too small to give a valid conclusion. Only two simulations with 200 bits each were used for the conclusions discussed here for smaller bandwidth systems.

Figures 18 and 19 can be compared in the same way as Figures 16 and 17. The Gaussian noise is the same for both figures. In this case the curve of Figure 19 does not level off but has a rather sharp minimum and then increases abruptly. In Figure 18, with less impulsive noise than in Figure 19, the optimum value of P is significantly higher than in Figure 19.

VII. CONCLUSIONS

The results presented here were obtained only for a small set of bandwidths and SNR's. Whether the results can be extrapolated to other bandwidths and SNR's is not known. However, if only the two bandwidths simulated are considered, it seems likely that the findings could be extended, with reasonably good results, to other signal to noise ratios. In the absence of large amounts of impulsive noise, it would seem reasonable to limit at a level of about 6 times $\sqrt{PSD}$ above the signal, for the $(10/\pi)$(Bit Rate BW) case. Of course, if a simulation of the particular situation is available, then one would simply use the optimum value of P.

There are a number of items which remain to be investigated. An analytic solution to the problem would be very desirable, and it may be possible to obtain. Also, perfectly coherent detection was assumed here. In practice the phase of the incoming signal must be estimated, and normally a device such as a phase-lock loop or a costas loop is used to make this estimate. The loss of lock in these systems due to impulsive noise could be considered.

For smaller bandwidth channels a matched filter for colored noise may give significantly better results, since it would be truly optimum for the Gaussian noise. A simulation could be done using this receiver in combinations of Gaussian and impulsive noise. Finally, incoherent receivers with optimum nonlinearities could be considered.

BIBLIOGRAPHY

[1] P.A. Bello and R. Esposito, "A new method for calculating probabilities of errors due to impulsive noise," IEEE Trans. on Communication Technology, Vol. COM-17, pp. 368-379, June 1969.

[2] L.R. Halsted, "On binary data transmission error rates due to combinations of Gaussian and impulsive noise," IEEE Trans. on Communications Systems, Vol. CS-11, pp. 428-435, December 1963.

[3] J.S. Engel, "Digital transmission in the presence of impulsive noise," Bell Sys. Tech. J., Vol. XLIV, pp. 1699-1743, October 1965.

[4] J.C. Lindenlaub and K.A. Chen, "Performance of matched filter receivers in non-Gaussian noise environments," IEEE Trans. on Communication Technology, Vol. COM-13, pp. 545-547, December 1965.

[5] R.E. Ziemer, "Character error probabilities for M-ary signaling in impulsive noise environments," IEEE Trans. on Communications Technology, Vol. COM-15, pp. 32-44, February 1967.

[6] R.E. Ziemer, "Error probabilities due to additive combinations of Gaussian and impulsive noise," IEEE Trans. on Communication Technology, Vol. COM-15, pp. 471-474, June 1967.

[7] C.W. Helstrom, Statistical Theory of Signal Detection, 2nd ed., New York: Pergamon Press, 1968.

[8] H.L. VanTrees, Detection, Estimation, and Modulation Theory, Part I. New York: Wiley, 1968.

[9] D. Middleton, An Introduction to Statistical Communication Theory. New York: McGraw-Hill, 1960.

[10] S. Thaler and S.A. Meltzer, "The amplitude distribution and false alarm rate of noise after post-detection filtering," Proceedings of the IRE, Vol. 49, pp. 479-485, February 1961.

[11] E.J. Baghdady, Ed., Lectures on Communication System Theory. New York: McGraw-Hill, 1961.

[12] H.V. Hogg and A.T. Craig, Introduction to Mathematical Statistics, 2nd ed., New York: Macmillan, 1965.

VITA

Ralph Bernard Fluchel was born on March 30, 1945, in St. Louis, Missouri. He received his primary and secondary education in Normandy, Missouri. He received a Bachelor of Science Degree in Electrical Engineering from the University of Missouri-Rolla in June, 1967.

He has been enrolled in the Graduate School of the University of Missouri-Rolla since September, 1967. During this time he has held a NASA Traineeship and a Graduate Research Assistantship in the Electrical Engineering Department.

The author is a member of Tau Beta Pi, Phi Kappa Phi, and Eta Kappa Nu.

APPENDIX A

Fortran Program For The Simulation

The program used in the simulation is presented here for reference. The program listed is for the system with a first order Butterworth filter. For this filter we have:

$$G_{bb}(t) = (\frac{B}{2}) \exp [- \frac{B}{2} t], \ 0, \leq t \leq T_o \quad . \tag{A-1}$$

where B is the bandwidth of g(t),

$$\phi_o(\tau) = \sigma^2 \exp [- \frac{B}{2} |\tau|] \ , \tag{A-2}$$

$$F_o(t) = \sqrt{\frac{2E}{T_o}} \ (1-\exp [- \frac{B}{2} t]), \ 0 \leq t \leq T_o \ . \tag{A-3}$$

It should be noted that the simulation could have been done for higher order filters. For example, for the second order butterworth filter we would use:

$$G_{bb}(t) = \frac{B\sqrt{2}}{2} \exp [- \frac{\sqrt{2}\ B}{4} t] \sin (\frac{\sqrt{2}\ B}{4} t), \ 0 \leq t \leq T_o \ , \tag{A-4}$$

$$F_o(t) = \sqrt{\frac{2E}{T}} - \sqrt{\frac{2E}{T}} \exp [- \frac{\sqrt{2}\ B}{4} t] \ x \ \{\sin \frac{\sqrt{2}\ B}{4} t + \cos \frac{\sqrt{2}\ B}{4} t\}$$

$$0 \leq t \leq T_o, \tag{A-5}$$

and

$$\phi_o(\tau) = \frac{1}{4(\frac{B^4}{16})} \exp [- \frac{B\sqrt{2}}{4} |\tau|] \ x \ \{\frac{B}{\sqrt{2}} \sin (\frac{\sqrt{2}\ B}{4} |\tau|) + \frac{B}{\sqrt{2}}$$

$$\cos (\frac{B\sqrt{2}}{4} |\tau|)\}. \tag{A-6}$$

The autocorrelation function was obtained by taking the inverse Fourier transform of the power spectral density and using contour integration to evaluate the integral.

The first part of the program generates the Gaussian noise samples for the simulation, using the approximation discussed in the thesis. A Gaussian random variable is approximated by adding twelve uniformly distributed random variables. This approximates a Gaussian random variable by the central limit theorem. The uniformly distributed random variable was generated by the power residue method as in the Scientific Subroutine Package for the IBM 360 computer.

Next, the times of occurrence of the noise impulses are computed. Since the number of occurrences, k, in any time, t_1, has a Poisson distribution:

$$P_{t_1}(k) = \frac{(ft_1)^k}{k!} \exp[-ft_1], \quad k = 0,1,... \tag{A-7}$$

then, letting t_2 be the length of time until the first occurrence, t_2 has an exponential p.d.f.:

$$g(t_2) = f\, e^{-ft_2}, \quad 0 \leq t_2 \leq \infty . \tag{A-8}$$

This is easy to show.

$$P[T_2 \leq t_1] = \int_0^{t_1} f\, e^{-ft_2}\, dt_2 = 1-e^{-ft_1} \tag{A-9}$$

$$P[T_2 > t_1] = 1-P[T_2 \leq t_1] = e^{-ft_1} \tag{A-10}$$

$$\text{But } P[T_2 > t_1] = P_{t_1}(0) = e^{-ft_1} \tag{A-11}$$

Since the probabilities are equal it must be concluded that $g(t_2) = f\, e^{-ft_2}$, $0 \leq t_2 \leq \infty$ is the correct p.d.f. Since the statistics are assumed stationary, the time of the last noise impulse occurrence can be taken to be zero, and then t_2 becomes the length of time between occurrences and has the same exponential p.d.f.

To obtain a random variable with an exponential distribution is a relatively simple matter as long as a uniformly distributed random variable can be obtained.

$$P[T_2 \leq t_2] = \int_0^{t_2} f\, e^{-f\tau}\, d\tau = 1-e^{-ft_2} \tag{A-12}$$

$$\text{But } P[T_2 \leq t_2] = F(t_2) \tag{A-13}$$

where $F(t_2)$ is the cumulative distribution function.

Define the random variable Z:

$$Z = F(T_2) \tag{A-14}$$

It can be shown ([12], p. 178) that Z has a uniform distribution on the interval [0,1].

Therefore:

$$F(T_2) = 1-e^{-ft_2} \sim \mu(0,1) \tag{A-15}$$

where $\sim$ denotes that the random variable on the left has the distribution on the right, and $\mu(0,1)$ is the uniform distribution on the interval [0,1].

Then:

$$-e^{-ft_2} \sim \mu(-1,0) \tag{A-16}$$

$$e^{-ft_2} \sim \mu(0,1) \tag{A-17}$$

$$\text{Let} \quad Z_1 = e^{-ft_2} \tag{A-18}$$

and $Z_1 \sim \mu(0,1)$. This equation can be solved for T_2:

$$T_2 = -\frac{1}{f} \ln Z_1 \tag{A-19}$$

Therefore, to get an exponentially distributed random variable, T_2, draw Z_1 from a uniformly distributed population on [0,1]. Then find T_2 by the above equation.

After finding the times of the noise impulses, their amplitudes are calculated, assuming the amplitudes have a Gaussian distribution. Next, the signal plus noise samples are multiplied by the baseband signal and the result is integrated using Simpson's rule. The result of the integration is compared with zero. If the result is less than zero an error is counted.

```
//*    LIMITS=(T=3,P=200)
C                PROBABABILITY  OF  ERROR  SIMULATION
C
      DIMENSION TDN(11), TD(10), AMPL(10), OUT(15), GAU(5600)
      COMMON TD,AMPL,IMAX,W0,B,C1,C2,C3,C4,C5,C6,C7,C,GAU,INK
      INTEGER TR(14)
      E=1.0
      W0=(2.0*3.141593*1.0E6)
      T0=(1.)/2000.
      B=2.*3.141593*2000.*3.185
      C1=SQRT(2.0*E/T0)
      C2=SQRT(2.)*B/4.0
      C3=B*SQRT(2.)/2.0
      C4=B/2.*SQRT(3.)
      C5=B/2.0
      C6=B/4.0
      C7=SQRT(3.)*B/4.0
      C8=8.*SQRT(3.)/21.
      TC=1./2000.
      TN=T0+TC
      NUMER=0
      IZERO=0
      IK=0
      JK=0
      KM=0
      R=EXP(-(B/2.)*(.0005/48.))
      PSD=0.254
      SIG=SQRT((3.141593/2.)*2000.*3.185*PSD)
      IX3=515733599
      AMP=0.0
      SIGM=SIG*SQRT(1.0-R*R)
   33 DO 100 NT=1,5555
      AG=0.0
      DO 500 I2=1,12
      IZ=IX3*65539
      IF(IZ) 405, 406, 406
  405 IZ=IZ+2147483647+1
  406 YFM=IZ*.46566135E-9
      IX3=IZ
  500 AG=AG+YFM
      VG=(AG-6.0)*SIGM+AMP
      GAU(NT)=VG
  100 AMP=VG*R
      INK=24
   30 JK=JK+1
      KM=KM+1
      I=0
      IF(JK-1) 21,21,20
   20 GO TO 22
   21 IX=1315206047
   22 TOT=0.0
    1 CALL RANDU (IX,IY,YFL)
      IX=IY
      I=I+1
      F1=200.0
      TDN(I)=-(1./F1)*ALOG(YFL)
      TOT=TOT+TDN(I)
      IF(TOT-TN) 1,2,2
    2 IF(I-1) 3,3,4
```

```
    3 IL=I-1
      TD(1)=0.0
      IMAX=1
      GO TO 101
    4 IF(I-11) 5,5,6
    5 IL=I-1
      DO 11 J=1,IL
C
C               TD(J)  ARE  OCCURRENCE  TIMES  OF  NOISE  IMPULSES
C
   11 TD(J)=TDN(J)-TC
      GO TO 8
    6 WRITE(3,7)
    8 IMAX=I
      KJ=IMAX-1
      DO 23 K=1,KJ
      IK=IK+1
      IF(IK-1) 18,18,19
   18 IX2=169807375
   19 AM=0.0
      SIGMA=0.0797
       CALL GAUSS(IX2,SIGMA,AM,V)
C
C               AMPL(I)  ARE  AMPLITUDES  OF  NOISE  IMPULSES
C
   23 AMPL(K)=V
C
C               INTEGRATION  BY  SIMPSON'S  RULE
C
  101 A=0.0
      A1=0.0005
      N=24
      L=0
 1001 L=L+1
      N=2*N
      H=(A1-A)/N
      W=A-H
      EVEN=0.
      ODD=0.
      VALI=F2(A)
      VALF=F2(A1)
      DO 1010 I=2,N,2
      W=W+(2.*H)
 1010 EVEN=EVEN + F2(W)*4.
      W=A
      K=N-1
      DO 1015 I=3,K,2
      W=W+(2.*H)
 1015 ODD=ODD + F2(W)*2.0
 1020 OUT(L)=(VALI+EVEN+ODD+VALF)*(H/3.)
      IF(OUT(L)) 35, 36, 1040
   35 NUMER=NUMER + 1
      GO TO 1040
   36 IZERO=IZERO + 1
 1040 CONTINUE
      IF(JK -100) 34,33,34
   34 IF(JK-200)30,31,31
   31 WRITE(3,32) IX,IX2,IX3
      RNUM=NUMER
```

```
      RZERO=IZERO
      RJK=JK
      PE=(RNUM + RZERO/2.0)/RJK
      DSNR = 20.0*ALOG10(SQRT(E/(PSD/2. + SIGMA*SIGMA*F1)))
      GPSD=PSD/2.0
      RIPSD=SIGMA*SIGMA*F1
      RATIO=RIPSD/(RIPSD + GPSD)
      WRITE(3,94) B
      WRITE(3,97) DSNR
      WRITE(3,98) RIPSD
      WRITE(3,99) GPSD
      WRITE(3,80) RATIO
      WRITE(3,96) PE
    7 FORMAT(10X, 'TOO MANY IMPULSES')
   32 FORMAT('1', 10X,'IX = ',I11//,10X,'IX2 = ',I11//,10X,'IX3 = ',
     2I11//)
   90 FORMAT(10X,I6,10X,F10.5)
   91 FORMAT('0',10X,'ANSWER',10X, I6, 10X, F10.5, 20X,'TRIAL',I7///)
   93 FORMAT('0', 10X, 'NUMBER OF IMPULSES = ', I2/)
   94 FORMAT('1',15X, 'SIMULATION RESULTS USING FIRST ORDER BUTTERWORTH
     1FILTER, LIMITER NO. 2, BANDWIDTH = ', F11.1,'   (1.00P)'///)
   95 FORMAT(10X,14I8)
   96 FORMAT('0', 30X, 'PROBABILITY OF ERROR = ', 2X, F13.9)
   97 FORMAT('0',30X,'SIGNAL TO NOISE RATIO DB = ', F6.1)
   98 FORMAT('0',30X,'BILATERAL PSD FOR IMPULSE NOISE = ', F9.4)
   99 FORMAT('0',30X,'BILATERAL PSD FOR GAUSSIAN NOISE =', F9.4)
   80 FORMAT('0',30X, 'RATIO OF IMPULSE NOISE TO TOTAL NOISE= ', F10.6)
      STOP
      END
      FUNCTION F2(T)
C
C                  LIMITER NUMBER 2
C
      E=1.0
      T0=(1.)/2000.
      P=SQRT(2.*E/T0)
      D1=SQRT(2.*E/T0)
      CALL SPN1(T,S)
      IF(S .GT. P) S=0.0
      IF(S .LT. -P) S=0.0
      F2=S*D1
      RETURN
      END
      SUBROUTINE SPN1(T,S)
C
C            FOR FIRST ORDER BUTTERWORTH FILTER
C
      DIMENSION TD(10), AMPL(10), GAU(5600)
      COMMON TD,AMPL,IMAX,W0,B,C1,C2,C3,C4,C5,C6,C7,C,GAU,INK
      GBB(T)=C5*EXP(-C5*T)
      INK=INK+1
      RNT=0.0
      NK=IMAX-1
      IF(NK .LT. 1) GO TO 2
      DO 1 I=1,NK
      RNI=AMPL(I)*COS(W0*TD(I))*GBB(T-TD(I))
      IF(T .LT. TD(I)) RNI=0.0
    1 RNT=RNT+RNI
    2 Z0=GAU(INK)


      Z1=C1
      Z2=-C1*EXP(-C5*T)
      S=RNT+Z0+Z1+Z2
      RETURN
      END
      SUBROUTINE RANDU(IX,IY,YFL)
      IY=IX*65539
      IF(IY) 5,6,6
    5 IY=IY+2147483647+1
    6 YFL=IY*.4656613E-9
      RETURN
      END
      SUBROUTINE GAUSS(IX,S,AM,V)
      A=0.0
      DO 50 I=1,12
      CALL RANDU(IX,IY,Y)
      IX=IY
   50 A=A+Y
      V=(A- 6.0)*S+AM
      RETURN
      END
/DATA
/END
```